



Université du Québec  
à Rimouski

**ENREGISTREMENT SÉDIMENTAIRE DE L'INFLUENCE  
DES BARRAGES SUR LA DYNAMIQUE DU FLEUVE  
NELSON ET DE LA RIVIÈRE CHURCHILL, OUEST DE LA  
BAIE D'HUDSON, AU COURS DES DERNIERS SIÈCLES**

Mémoire présenté  
dans le cadre du programme de maîtrise en océanographie  
en vue de l'obtention du grade de maître ès sciences

PAR  
© QUENTIN DUBOC

Juillet 2015



**Composition du jury :**

**André Rochon, président du jury, Université du Québec à Rimouski**

**Guillaume St-Onge, directeur de recherche, Université du Québec à Rimouski**

**Patrick Lajeunesse, codirecteur de recherche, Université Laval**

**Emmanuel Chapron, examinateur externe, Université de Toulouse**

Dépôt initial le 15 janvier 2015

Dépôt final le 8 juillet 2015



UNIVERSITÉ DU QUÉBEC À RIMOUSKI  
Service de la bibliothèque

Avertissement

La diffusion de ce mémoire ou de cette thèse se fait dans le respect des droits de son auteur, qui a signé le formulaire « *Autorisation de reproduire et de diffuser un rapport, un mémoire ou une thèse* ». En signant ce formulaire, l'auteur concède à l'Université du Québec à Rimouski une licence non exclusive d'utilisation et de publication de la totalité ou d'une partie importante de son travail de recherche pour des fins pédagogiques et non commerciales. Plus précisément, l'auteur autorise l'Université du Québec à Rimouski à reproduire, diffuser, prêter, distribuer ou vendre des copies de son travail de recherche à des fins non commerciales sur quelque support que ce soit, y compris l'Internet. Cette licence et cette autorisation n'entraînent pas une renonciation de la part de l'auteur à ses droits moraux ni à ses droits de propriété intellectuelle. Sauf entente contraire, l'auteur conserve la liberté de diffuser et de commercialiser ou non ce travail dont il possède un exemplaire.



## REMERCIEMENTS

Avant tout, je souhaite sincèrement remercier mon directeur de recherche, Guillaume St-Onge, qui m'a guidé dans mes travaux de recherche durant plus de deux années en m'accordant une confiance et un temps précieux. Merci également à mon codirecteur Patrick Lajeunesse pour son implication dans cette recherche, ainsi qu'à son étudiant Alexandre Normandeau pour l'aide précieuse qu'il a apporté dans la sélection des sites d'échantillonnage. Je remercie aussi Jacques Labrie, Marie-Pier St-Onge et Mathieu Babin pour leur aide en laboratoire à l'ISMER. Remerciements spéciaux à Gilles Desmeules, pour m'avoir accompagné à Churchill et sur le NGCC Pierre Radisson, alors que je ne savais rien des manipulations à bord. Finalement, un grand merci à Elissa Barris et Julie Velle pour les nombreuses heures qu'elles ont passées à corriger mon anglais encore lacunaire !

En 2 années, nous côtoyons beaucoup de personnes qui nous accompagnent, nous aident, nous soutiennent, et partagent notre vie de diverses façons... Pour cela, je remercie tout d'abord mes collègues et amis de l'équipe de recherche encore non cités : Pierre-Arnaud, Charles, Quentin, Marie, Audrey, Édouard et notamment Matthieu avec qui j'ai fait presque tout mon parcours ! Un gros merci également à Aurore, Julien, Kévin, Melany et Robin, mais aussi tous les autres étudiants qui ont animé ma vie à l'ISMER et au NÉMO! Une pensée également pour Sylvain et Marilou, pour Mathilde, Marion et Idaline, Vincent, et en particulier à Jamilie, pour tout ce précieux temps passé à leurs côtés hors des murs de l'UQAR. Merci bien sûr à mes parents, pour m'encourager sans arrêt qu'importent mes prises de décisions. Finalement, parce que tout cela aurait été difficile sans un bon carburant, j'envoie des becs aux serveuses (et au serveur) du café l'Auriculaire pour les litres de cafés qu'ils m'ont servis pendant ma rédaction !



## RÉSUMÉ

Deux carottes à gravité (778 et 780) échantillonnées à l'embouchure du fleuve Nelson, et une (776) à celle de la rivière Churchill, à l'ouest de la baie d'Hudson, Canada, ont été analysées dans le but d'identifier l'influence des modifications anthropiques (barrages, détournements de rivières) sur l'hydrologie des rivières et la dynamique sédimentaire. Une autre carotte (772) a été échantillonnée au large et utilisée comme carotte de référence qui n'est pas directement affectée par le régime des rivières. La chronologie des carottes a été établie à l'aide d'âges  $^{14}\text{C}$  et de mesures de  $^{210}\text{Pb}$ . La carotte 772 couvre les derniers 1800 ans et son homogénéité montre qu'elle ne contient pas de couche déposée rapidement. Les carottes 778 et 780 présentent plus de variations et les propriétés physiques, chimiques, magnétiques et sédimentologiques mesurées sur ces carottes révèlent la présence de plusieurs hyperpycnites, indiquant que des courants hyperpycnaux ont été formés lors de crues du fleuve Nelson. Ces courants ont probablement été générés par la formation d'embâcles qui causent une augmentation du débit et de la concentration de sédiment à la suite de leur rupture. Ces hyperpycnites ne sont cependant présentes que dans la partie inférieure des carottes. La remobilisation de sédiments par les crues empêche l'établissement d'une chronologie précise pour ces carottes. Toutefois, certaines dates  $^{14}\text{C}$  récentes suggèrent que le changement de structure est contemporain au harnachement du fleuve Nelson qui a débuté dans les années 1960 et qui permet un contrôle de son débit. Ainsi, cette régulation par les barrages empêche la formation de courants hyperpycnaux en aval et donc le dépôt d'hyperpycnites. Finalement, la carotte 776 couvre une période de 350 ans et ne contient qu'une seule couche déposée rapidement. Cette faible fréquence pourrait être expliquée par l'estuaire fermé de la rivière Churchill, la position au large du site de carottage et par son débit beaucoup moins élevé que celui du fleuve Nelson.

Mots clés : hyperpycnite, courant hyperpycnal, rivière, embâcle, crue, barrage hydroélectrique, impact anthropique.

## ABSTRACT

Two gravity cores (778 and 780) sampled at the Nelson River mouth and one (776) at the Churchill River mouth in western Hudson Bay, Canada, were analyzed in order to identify the anthropogenic impact on hydrology and sedimentary regime of both rivers, such as dam construction and river diversion. Another core (772) was sampled offshore and used as a reference core without a direct river influence. Core chronology was established using  $^{14}\text{C}$  and  $^{210}\text{Pb}$  measurements. Core 772 covers the last 1800 years and its homogeneity indicates that it is not affected by rapidly deposited layers. Cores 778 and 780 show greater variability, and the physical, chemical, magnetic and sedimentological properties measured on these cores reveal the presence of several hyperpycnites, indicating the occurrence of hyperpycnal flows due to floods of the Nelson River. These hyperpycnal flows were probably caused by ice-jam formation, which can increase both the flow and the sediment concentration following the breaching of such natural dam. However, these hyperpycnites are only located in the lower parts of cores 778 and 780. It was not possible to establish a precise chronology due to the remobilization of sediments by the floods. Nevertheless, some modern  $^{14}\text{C}$  ages suggest that this change in sedimentary regime is concurrent with the dam construction on the Nelson River, which allows a continuous control of its flow since the 1960s. In addition, the regulation of river discharge by the dams prevented the formation of hyperpycnal flows, and the deposition of hyperpycnites. Finally, core 776 covers a period shorter than the last 350 years and contains only one hyperpycnite. The lower frequency of hyperpycnal flows in core 776 may be due to the enclosed estuary of Churchill River, its weaker discharge and the distance of the site from shore.

*Keywords:* hyperpycnite, hyperpycnal flow, river, ice-jam, flood, hydroelectric dam, anthropogenic influence.

## TABLE DES MATIÈRES

REMERCIEMENTS .....	vii
RÉSUMÉ .....	ix
ABSTRACT .....	x
TABLE DES MATIÈRES .....	xi
LISTE DES TABLEAUX .....	xiii
LISTE DES FIGURES .....	xiv
INTRODUCTION GÉNÉRALE .....	1
PROBLEMATIQUE .....	1
OBJECTIFS DE LA RECHERCHE .....	3
EXPEDITION ET METHODOLOGIE .....	3
ORGANISATION DU MÉMOIRE ET CONTRIBUTION .....	5
PRESENTATIONS OFFICIELLES LORS DE CONGRES .....	6
CHAPITRE 1 Sediment records of climatic and river damming on the dynamics of the Nelson and Churchill Rivers, western Hudson Bay, Canada, during the last centuries .....	9
1. INTRODUCTION .....	9
2. REGIONAL SETTING .....	10
3. SAMPLING AND METHODS .....	12
3.1. Sampling .....	12
3.2. Physical analyses .....	13
3.3. Grain-size analyses .....	14
3.4. Magnetic analyses .....	14
3.5. Chemical analyses .....	15
3.6. Chronology .....	15
4. RESULTS .....	18

4.1.	Core top correlation.....	18
4.2.	Lithology .....	19
4.3.	Rock-magnetic data.....	24
4.4.	Chronology.....	25
5.	DISCUSSION.....	28
5.1.	Environmental changes since the last 1800 years .....	28
5.2.	Rapidly deposited layers .....	28
5.3.	Impact of river damming on the Nelson River dynamics .....	32
6.	CONCLUSIONS .....	33
	CONCLUSION GÉNÉRALE .....	34
	RÉFÉRENCES BIBLIOGRAPHIQUES .....	37
	ANNEXE 1 COORDONNÉES D'ÉCHANTILLONNAGE ET LEVÉS SISMIQUES .....	43

**LISTE DES TABLEAUX**

<b>Table 1.</b> Coordinates of the cores collected in southwestern Hudson Bay.....	13
<b>Table 2.</b> AMS $^{14}\text{C}$ dated material and results.....	17

## LISTE DES FIGURES

<b>Figure 1.</b> Carte de la baie d'Hudson et localisation des stations d'échantillonnage. ....	4
<b>Figure 2.</b> (A) Carottier à gravité et (B) Carotte 776 échantillonnée avec le carottier à gravité.....	5
<b>Figure 3.</b> (A) Carottier à boîte, (B) Carotte à boîte (772) contenant l'interface eau/sédiment et (C) <i>Push-cores</i> contenant des duplicates de la carotte à boîte (772). ....	5
<b>Figure 4.</b> River drainage in the Hudson Bay watershed with the location of the sampled cores (in blue) and the cores from Kuzyk et al. (2009) referred in this paper (in black). The location of Hudson Bay in North America is in the top-right corner. The largest red area is the part of the Churchill watershed that was diverted to the Nelson river system in 1976. Modified from Stewart and Lockhart (2005). .....	12
<b>Figure 5.</b> Correlation (magnetic susceptibility $k_{LF}$ or Fe content) between the <i>LeHigh</i> gravity core (leh; in red) and the box-core (BC; in black) for the four sites sampled. Even though the Fe results are presented as ppm, only relative changes were used here as an absolute calibration with sediments was not performed. ....	18
<b>Figure 6.</b> X-Ray image and derived grey scale values, physical, sedimentological, magnetic and geochemical properties of core 772 versus depth. ....	19
<b>Figure 7.</b> X-Ray image and derived grey scale value, physical, sedimentological, magnetic and geochemical properties of core 776 versus depth. ....	20
<b>Figure 8.</b> X-Ray image and derived grey scale value, physical, sedimentological, magnetic and geochemical properties versus depth for the gravity cores of sites <b>A</b> ) 778 and <b>B</b> ) 780, with the non-corrected depths. The $^{14}\text{C}$ ages are indicated. The RDL are highlighted in grey and the upper part in yellow.....	22
<b>Figure 9.</b> Comparison between cores 778 and 780 with the density and the $k_{ARM}/k$ ratio after depth correction to account for the missing sediment in the upper part of the cores. The RDL are highlighted in grey, whereas the upper variations are in yellow.....	23
<b>Figure 10.</b> Hysteresis curves and derived parameters of a representative sample from each core 772 ( <b>A</b> ), 776 ( <b>B</b> ) and 778 ( <b>C</b> ), and 2 samples from core 780 ( <b>D</b> and <b>E</b> ). In	

D), the sample is from finer background sediments, while in E) it is from a coarser RDL ..... 24

**Figure 11.**  $^{210}\text{Pb}$  measurements for the four cores with the derived sedimentation rate (SR). Biological mixing occurs in cores 776, 778 and 780. The regional supported  $^{210}\text{Pb}$  is determined by the trend of  $^{210}\text{Pb}$  in core 772 ..... 25

**Figure 12.** Age-model of core 772 based on the  $^{14}\text{C}$  age and  $^{210}\text{Pb}$  data. ..... 26

**Figure 13.** Representation of a river with A) an ice-jam, B) a subsequent hyperpycnal flow and C) hydroelectric dams that prevent the floods ..... 31



## INTRODUCTION GÉNÉRALE

### **Problématique**

Les rivières, fleuves et autres cours d'eau sont perpétuellement soumis aux variations de température et de précipitation, ce qui en font de très bons témoins des variations climatiques touchant les régions associées. Les changements climatiques des dernières décennies, généralement associés à une hausse des températures globales, suscitent questionnements et inquiétudes et sont sources de nombreuses études sur la connexion entre les paramètres climatiques et l'écoulement des rivières (p.ex. Burn, 1994 ; Beltaos and Burrell, 2003 ; St-Jacques et al., 2010). Dans ce contexte, l'étude des variations passées des cours d'eau est primordiale pour déterminer l'influence du climat sur celles-ci. Pour cela, les carottes sédimentaires sont de très bons outils car les propriétés sédimentaires, en particulier la granulométrie, permettent de retracer la dynamique du courant en un lieu précis à travers le temps (p.ex. Starkel, 2011 ; Boyer-Villemaire et al., 2013). Ainsi, échantillonnées à l'embouchure de rivières, les carottes renseignent sur les fluctuations du débit de celles-ci au cours du temps et permettent d'identifier des événements majeurs tels que les crues (Starkel, 2002 ; Werritty et al., 2006 ; Mulder & Chapron, 2010). Dans le secteur de la baie d'Hudson, grande mer intérieure localisée au centre du Canada et ouverte sur l'Arctique, les récents changements climatiques se traduisent généralement par une diminution du débit annuel des cours d'eau, un gel plus tardif et une débâcle plus hâtive (Burn, 1994; Déry et al., 2005). Il devrait donc être possible d'identifier cette évolution dans des carottes sédimentaires récupérées aux embouchures de rivières situées en baie d'Hudson.

Cependant, de nombreux cours d'eau de ce secteur ont été harnachés, généralement dans le but de combler les besoins en électricité des provinces avoisinantes (Anctil & Couture, 1994; Déry & Wood, 2005). Plusieurs études ont déjà démontré que les activités humaines, telles que la mise en place de barrages ou la déforestation, ont des impacts majeurs sur la dynamique naturelle des cours d'eau (p.ex. Vörösmarty et al., 2003 ; Valiela et al., 2014). Ainsi, l'implantation de barrages hydroélectriques sur un cours d'eau permet

d'en contrôler le débit en fonction des besoins en électricité, entraînant généralement une homogénéisation du régime hydrologique du cours d'eau en aval et des conséquences sur les écosystèmes (Poff et al., 2007). De plus, les réservoirs en amont du barrage font office de trappes à sédiments et l'apport de matériel à l'embouchure a tendance à diminuer (Vörösmarty et al., 2003). Le transport sédimentaire peut donc être modifié au point de camoufler, voire supprimer, le signal climatique qu'il serait normalement possible de retrouver dans les carottes sédimentaires échantillonnées en aval (Boyer-Villemaire et al., 2013).

La rivière Churchill et le fleuve Nelson, dont les embouchures sont situées à l'ouest de la baie d'Hudson (nord du Manitoba) sont de bons exemples d'importants cours d'eau récemment harnachés. Ils contribuent à eux seuls à 20% des apports d'eau douce de la baie d'Hudson et leurs bassins versants s'étendent sur 4 provinces canadiennes et 4 états américains (Rosenberg et al., 2005 ; Kuzyk et al., 2009). La dynamique de la rivière Churchill et du fleuve Nelson pourrait donc être affectée par les variations du climat telles que celles engendrées par les oscillations climatiques, principalement l'El Niño-oscillation australe (ENSO) et l'oscillation décennale du Pacifique (PDO) qui influencent le climat de l'ouest et du centre du pays (Bonsal & Shabbar, 2011). Cependant, ces cours d'eau ont été aménagés dès les années 1960 pour tirer profit de leurs hauts débits : 5 barrages ont été construits sur le fleuve Nelson et 75 à 85% des eaux de la rivière Churchill ont été détournées dans le chenal de celui-ci pour optimiser au maximum la production hydroélectrique (Manitoba Wildlands, 2005 ; Rosenberg et al., 2005). Ce détournement a considérablement modifié le débit moyen des deux cours d'eau, augmentant de  $2240 \text{ m}^3/\text{s}$  à  $3050 \text{ m}^3/\text{s}$  pour le fleuve Nelson et diminuant de  $1350 \text{ m}^3/\text{s}$  à  $600 \text{ m}^3/\text{s}$  pour la rivière Churchill (Rosenberg et al., 2005). De plus, les barrages permettent de réguler le débit du fleuve Nelson et de contrôler les crues causées principalement lors de la débâcle printanière, régularisant ainsi l'hydrogramme du fleuve qui ne répond plus à la variabilité naturelle du climat (Anctil & Couture, 1994 ; Rosenberg et al., 2005).

## Objectifs de la recherche

L'objectif principal de cette maîtrise est de reconstituer les variations récentes de la dynamique du fleuve Nelson et de la rivière Churchill, ainsi que d'identifier l'impact des modifications anthropiques sur la dynamique de ces cours d'eau par rapport à la variabilité naturelle. Plus précisément, il s'agit tout d'abord d'étudier des carottes sédimentaires afin d'identifier des variations ou des couches déposées rapidement à l'aide de structures sédimentaires et/ou de leurs propriétés physiques, magnétiques, sédimentologiques et géochimiques. Ensuite, la chronologie de ces changements devra être établie afin de les associer à des facteurs climatiques (oscillations climatiques) et/ou anthropiques (barrages et détournement de rivière).

## Expédition et méthodologie

L'échantillonnage des carottes utilisées pour l'étude a été réalisé à bord du NGCC Pierre Radisson au cours de l'été 2012. Le départ et le retour se sont faits à Churchill, ville située au nord du Manitoba sur la côte ouest de la baie d'Hudson (Figures 1 et 4). Les sites de carottage avaient été préalablement sélectionnés par Alexandre Normandeau à l'Université Laval à partir de données sismiques provenant de précédentes expéditions réalisées dans le cadre du programme ArcticNet. Le premier site carotté (PRAD121-772) était situé à 200 km au large des embouchures des rivières (Figures 1 et 4). Ensuite, 2 sites ont été échantillonnés à proximité de l'embouchure du fleuve Nelson (PRAD121-778 et PRAD121-780), et le dernier site était localisé près de l'embouchure de la rivière Churchill (PRAD121-776). À chaque site, un carottier à gravité *Lehigh* de 3 m a été utilisé (Figure 2), ainsi qu'un carottier à boîte (Figure 3). L'utilité de ce dernier était d'obtenir un échantillon de l'interface eau-sédiment, au cas où celle-ci n'aurait pas été préservée dans la carotte à gravité, l'impact du carottier à gravité pouvant la détruire.

Les carottes ont ensuite été acheminées à l'ISMER où des radiographies digitales ont d'abord été réalisées. Elles ont ensuite été soumises à une série d'analyses physiques, chimiques et magnétiques à l'aide d'un *Multi Sensor Core Logger* (MSCL) et d'un

magnétomètre cryogénique. Des échantillons ont été récoltés tous les 4 cm sur les carottes à gravité pour effectuer des analyses granulométriques, géochimiques (C et N) et isotopiques ( $^{13}\text{C}$ ). Le ratio magnétique  $k_{\text{ARM}}/k$  et le ratio géochimique Zr/Rb, qui sont tous deux intimement liés à la taille des grains (p.ex., Croudace et al., 2006; Stoner et St-Onge, 2007), ont été calculés pour supporter les analyses granulométriques. Finalement, la chronologie a été établie à l'aide d'âges  $^{14}\text{C}$  obtenus sur des fragments de coquilles et des mesures de  $^{210}\text{Pb}$ .

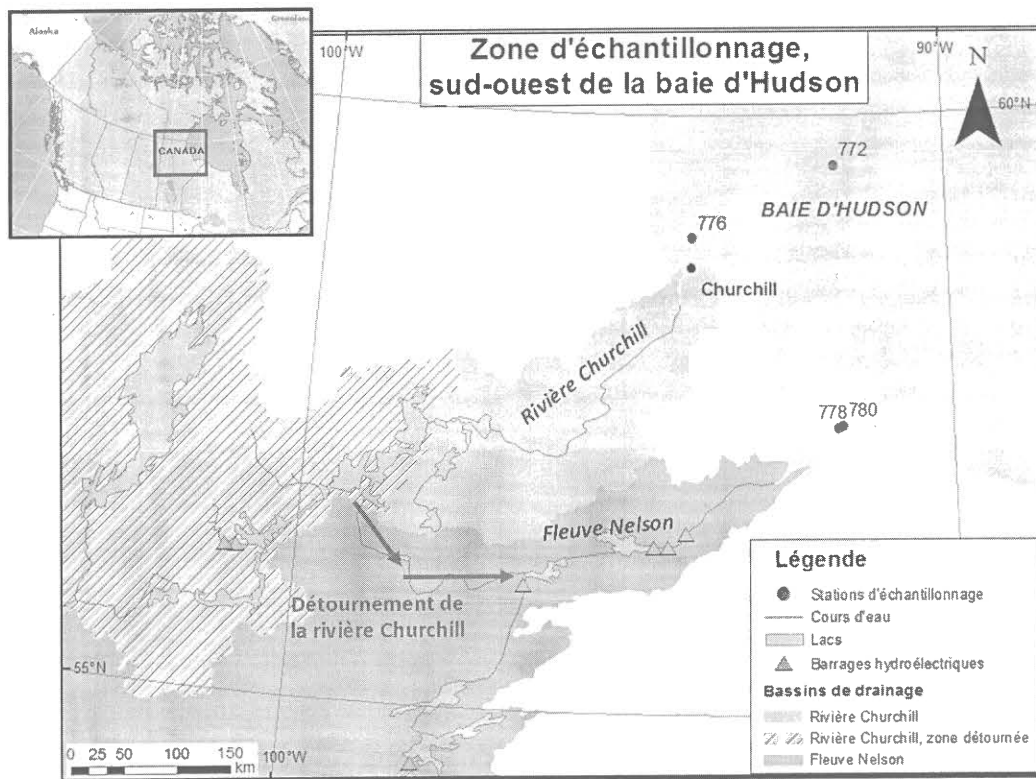


**Figure 1.** Carte de la baie d'Hudson et localisation des stations d'échantillonnage.

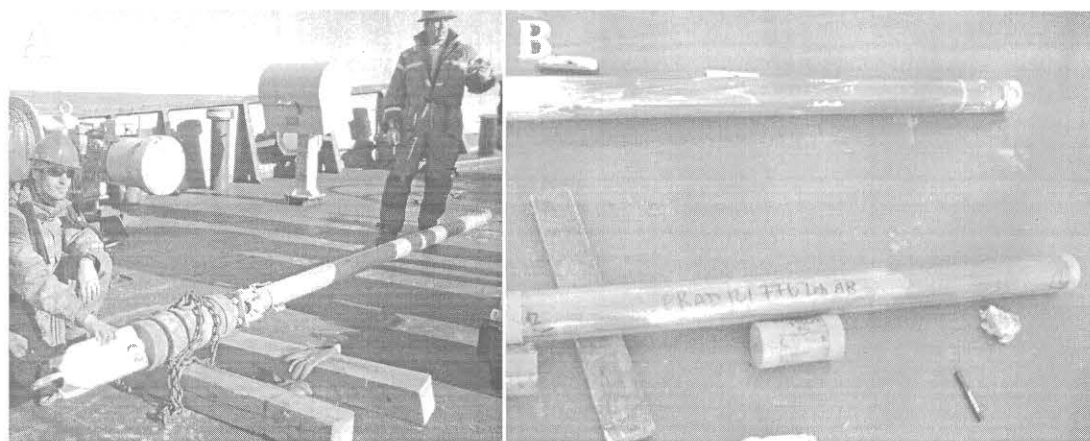


**Figure 2.** (A) Carottier à gravité et (B) Carotte 776 échantillonnée avec le carottier à gravité.

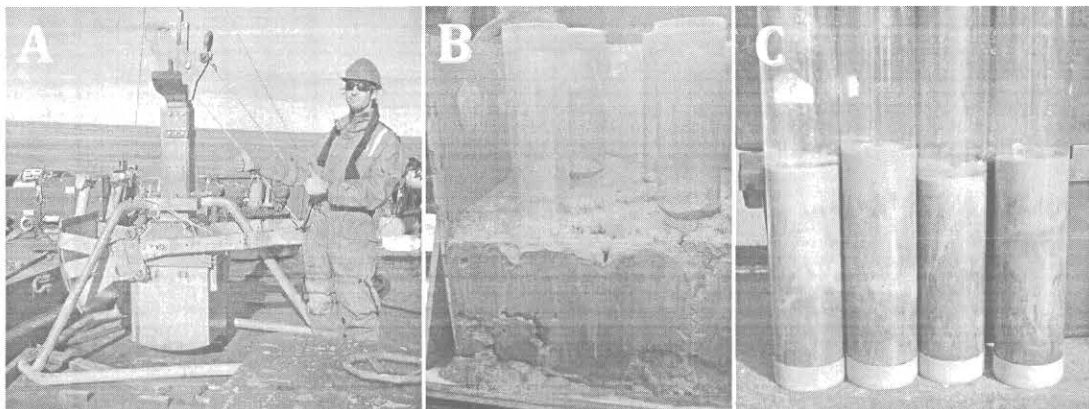


**Figure 3.** (A) Carottier à boîte, (B) Carotte à boîte (772) contenant l'interface eau/sédiment et (C) Push-cores contenant des duplicates de la carotte à boîte (772).

### Organisation du mémoire et contribution

Ce mémoire de maîtrise est rédigé en anglais sous forme d'article scientifique qui sera soumis prochainement à la revue *The Holocene* sous la référence :

**Duboc, Q., St-Onge, G., Lajeunesse, P., sera soumis prochainement. Sediment records of the influence of river damming on the dynamics of the Nelson and Churchill Rivers, western Hudson Bay, Canada, during the last centuries. *The Holocene.***

Dans le cadre de ce mémoire de maîtrise, j'ai participé à l'échantillonnage des carottes à la fin de l'été 2012 et j'ai effectué toutes les analyses en laboratoire à l'exception des analyses isotopiques et élémentaires ainsi que celles de  $^{14}\text{C}$  et de  $^{210}\text{Pb}$  qui ont respectivement été faites à l'Université Laval/UC Irvine et au GEOTOP à Montréal. Je me suis également chargé du traitement et de l'interprétation des données, ainsi que de la rédaction de l'article et du mémoire. Guillaume St-Onge et Patrick Lajeunesse ont tous deux apporté leur soutien à la réalisation de ce mémoire de maîtrise par leur aide et expertise précieuse en géologie marine, sédimentologie et géomorphologie. De plus, les deux ont contribué aux diverses versions préliminaires de l'article scientifique.

### **Présentations officielles lors de congrès**

Au cours de ma maîtrise, j'ai eu la chance de participer à plusieurs congrès scientifiques. À chacun d'eux, j'y ai présenté un ou plusieurs aspects de ma recherche sous forme d'affiches ou de présentations orales. Voici la liste de mes présentations :

**Duboc, Q., St-Onge, G., Lajeunesse, P., 2013. Magnetic field changes and stratigraphy of southwestern Hudson Bay sediments. Affiche lors du congrès du GEOTOP, 1-3 février 2013, Wentworth-Nord (QC), Canada.**

**Duboc, Q., St-Onge, G., Lajeunesse, P., 2013. Paleomagnetism and environmental changes from southwestern Hudson Bay Holocene sediments: preliminary results. Affiche lors du 43rd Annual International Arctic Workshop, 11-13 mars 2013, Amherst (MA), USA.**

**Duboc, Q., St-Onge, G., Lajeunesse, P.,** 2014. Magnetic field and environmental changes in the western Hudson Bay during the last 1700 years. Présentation orale lors du congrès du GEOTOP, 14 au 16 mars 2014 à Pohénégamook (QC), Canada.

**Duboc, Q., St-Onge, G., Lajeunesse, P.,** 2014. Recent flood events of the Nelson and Churchill Rivers and environmental changes since the last 1700 years in western Hudson Bay. Affiche lors du 48<sup>ème</sup> congrès de la Société Canadienne de Météorologie et d'Océanographie (SCMO), 1-5 juin 2014 à Rimouski (QC), Canada.

**Duboc, Q., St-Onge, G., Lajeunesse, P.,** 2014. Rapidly deposited layers from Western Hudson Bay (Canada): a record of major floods from the Nelson and Churchill Rivers in the last 500 years. Affiche lors du 19<sup>ème</sup> *International Sedimentological Congress*, 18-22 août 2014 à Genève, Suisse.

**Duboc, Q., St-Onge, G., Lajeunesse, P.,** 2014. Rapidly deposited layers from Western Hudson Bay: a possible record of floods from the Nelson and Churchill Rivers in the last 700 years. Présentation orale lors du congrès *Arctic Change 2014*, 8-12 décembre 2014 à Ottawa (ON) Canada.

**Duboc, Q., St-Onge, G., Lajeunesse, P.,** 2015. Rapidly deposited layers from Western Hudson Bay: a possible record of floods from the Nelson and Churchill Rivers in the last 700 years. Présentation orale lors du congrès du GEOTOP, 13 au 15 février 2015 à Pohénégamook (QC), Canada.

**Duboc, Q., St-Onge, G., Lajeunesse, P.,** 2015. Enregistrements sédimentaires de la dynamique du fleuve Nelson et de la rivière Churchill, ouest de la baie d'Hudson, au cours des derniers siècles. Présentation orale lors du congrès *ACFAS 2015*, 25-29 mai 2015 à Rimouski (QC) Canada.



# CHAPITRE 1

## SEDIMENT RECORDS OF THE INFLUENCE OF RIVER DAMMING ON THE DYNAMICS OF THE NELSON AND CHURCHILL RIVERS, WESTERN HUDSON BAY, CANADA, DURING THE LAST CENTURIES

**Quentin Duboc<sup>a,b</sup>, Guillaume St-Onge<sup>a,b</sup> et Patrick Lajeunesse<sup>c</sup>**

<sup>a</sup> Institut des sciences de la mer de Rimouski (ISMER), Canada Research Chair in Marine Geology, Université du Québec à Rimouski, Rimouski, Canada

<sup>b</sup>GEOTOP Research Center, Canada

<sup>c</sup>Centre d'études nordiques (CEN) & Département de Géographie, Université Laval, Québec, Canada

### **1. Introduction**

Several studies have demonstrated that sediment transport in rivers is highly impacted by anthropogenic activities such as damming, river diversion or deforestation (e.g., Syvitski et al., 2005; Yang et al., 2006; Valiela et al., 2014). In particular, the construction of hydroelectric dams can affect the rivers' hydrology and sediment dynamics that would otherwise be governed by climatic variations (e.g., Boyer-Villemaire et al., 2013). This anthropogenic influence may be identified in sediment cores sampled in estuarine environments as they provide a continuous record of variations in currents and/or in river dynamics (e.g. Macklin & Lewin, 2003; Vannière et al., 2013).

In Canada, many rivers are characterized by seasonal dynamics due to the presence of river-ice during the winter. In spring, the flow increases and the break-up of the ice, sometimes followed by ice-jam formation, may trigger major floods downstream (Beltaos & Prowse, 2001). However, hydroelectric installations, which are common in Canada,

take advantage of the increased flow and allow a control of the river floods. The Nelson and Churchill Rivers are examples of large Canadian rivers that are subject to anthropogenic modifications as they were dammed during the second half of the 20<sup>th</sup> century (Anctil & Couture, 1994; Manitoba Wildlands, 2005). Since the construction of these dams, the Nelson River flow is regulated to avoid floods and extensive ice-jamming no longer occurs in the lower Nelson River (Rosenberg et al., 2005). Moreover, the Churchill River was diverted to the Nelson River channel in 1976 to take advantage of its great hydroelectric potential (Newbury et al., 1984; Manitoba Wildlands, 2005), significantly increasing the Nelson River flow from 2240 to 3050 m<sup>3</sup>/s and reducing the Churchill River flow from ~1350 to ~600 m<sup>3</sup>/s (Prisenberg, 1980; Déry et al., 2011). In this study, sediment cores sampled near the mouth of these rivers are used to investigate the impact of anthropogenic modifications on the rivers' hydrodynamics. Another core, sampled farther offshore, serves as a reference core without direct river influence.

## 2. Regional setting

Hudson Bay is a large and shallow Canadian inland sea located between four Canadian provinces and territories: Nunavut (to the west), Manitoba and Ontario (to the south) and Quebec (to the east) (Fig. 4) (Stewart & Lockart, 2005). During the Last Glacial Maximum (18 ka BP), Hudson Bay was completely covered by the Laurentide Ice Sheet (LIS) (Dyke, 2004). The progressive deglaciation allowed the formation of the large proglacial Lake Agassiz-Ojibway at the southern margin of the LIS (e.g., Barber et al., 1999; Lajeunesse & St-Onge, 2008). Around 8470 cal BP, the catastrophic drainage of the Lake Agassiz-Ojibway beneath the LIS into the Tyrrell Sea (Hudson Bay precursor) led to the final failure of the ice-jam and to the formation of a sequence of two hyperpycnal deposits (hyperpycnites) associated with this major flood (St-Onge and Lajeunesse, 2007; Lajeunesse & St-Onge, 2008). Since then, the coast of Hudson Bay has been emerging as a result of glacio-isostatic rebound (Stewart & Lockart, 2005), and this continental uplift continues today at a mean rate of 8-10 mm/yr (Sella et al., 2007). At present, Hudson Bay covers an area of 841 000 km<sup>2</sup> with a mean depth of only 125 m and

a seabed slope of generally less than 2° (Kuzyk et al., 2009). It experiences each year a complete sea-ice cover and receives 30% of the total Canadian freshwater runoff (Déry et al., 2005).

Two major rivers, the Nelson and Churchill Rivers, enter western Hudson Bay on the coast of Manitoba. The Nelson River is the third largest river in Canada, contributing to 16.3% of the freshwater inflow to Hudson Bay. Its drainage basin covers an area of 1 125 520 km<sup>2</sup>, from the Rocky Mountains in the west to Ontario in the east and Minnesota and South Dakota in the south (Rosenberg et al., 2005; Kuzyk et al., 2009). Its average annual mean discharge is 3050 m<sup>3</sup>/s, but can reach ~6500 m<sup>3</sup>/s during spring freshet (Rosenberg et al., 2005; Kirk & St-Louis, 2009). The Churchill River basin, located north of Nelson River's basin, is smaller and includes 281 300 km<sup>2</sup> of Canadian land (Rosenberg et al., 2005). Unlike the Nelson River, whose mouth forms an open estuary, the Churchill River ends in a 13 km long enclosed estuary with a weir located at the upstream end (Kuzyk et al., 2008). Before the hydro-development, the lower Nelson River was covered with ice each winter from its mouth and up to 250 km upstream, and the spring freshet often triggered extensive ice-jams downstream on several kilometers (Rosenberg et al., 2005; North/South Consultants Inc., 2012). The first hydroelectric development was completed in 1928 on the Churchill River (Anctil & Couture, 1994) and in 1961 on the main section of the Nelson River. Five dams exist today between Lake Winnipeg and the mouth of the Nelson River. The last one, the Limestone Generating Station, is located 80 km before the river mouth (North/South Consultants Inc., 2012). These structures have divided the river channel into a series of flooded valley reservoirs that freeze early in the autumn and reduced the amount of ice brought downstream at the breakup, preventing extensive ice-jamming (Rosenberg et al., 2005; North/South Consultants Inc., 2012). Furthermore, in 1976, 75 - 85% of the natural flow of the Churchill River was diverted to the Nelson River channel to increase hydropower efficiency (Manitoba Wildlands, 2005; Rosenberg et al., 2005), disturbing the natural flow of both rivers (Prinsenberg, 1980; Anctil & Couture, 1994) and generating environmental complications such as severe erosion of frozen soils and increasing mercury levels in flooded lakes (Newbury et al., 1984; Bodaly et al., 1984).

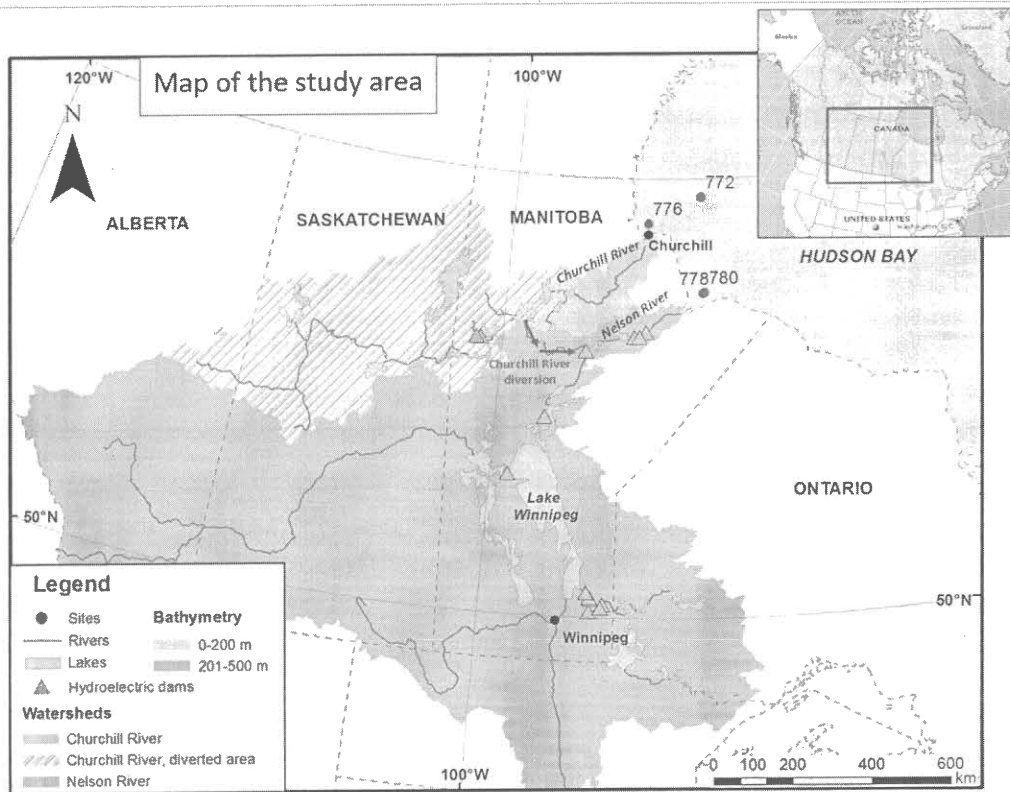


**Figure 4.** Map of the study area with the sampling sites and the watersheds of the Churchill and Nelson Rivers.

### 3. Sampling and methods

#### 3.1. Sampling

In the summer of 2012, four sites were cored on board the CCGS Pierre Radisson in southwestern Hudson Bay as part of the BaySys 2012 expedition carried out in the framework of the ArcticNet program (Table 1). These sites were selected for their apparent sediment thickness and their undisturbed surface based on seismic data collected from previous expeditions of the CCGS Amundsen in Hudson Bay. At each site, one Lehigh gravity core and one box core were sampled, and four push cores were sampled from each box core to obtain duplicates. Three of the sites are located near the coast of

Manitoba: site PRAD121-776 is near the Churchill River mouth, whereas sites PRAD121-778 and PRAD121-780 are near the Nelson River mouth. The fourth site, PRAD121-772, is about 200 km to the northeast (Fig 4). The cores will be hereinafter referred to as cores 776, 778, 780 and 772.

**Table 1.** Coordinates of the cores collected in southwestern Hudson Bay.

Site	Core	Latitude (°)	Longitude (°)	Water depth (m)
PRAD121-772	leh	59.5785	-91.816	131
	BC	59.5785	-91.8158	129
PRAD121-776	leh	58.9724	-94.0986	49.5
	BC	58.9724	-94.0983	49
PRAD121-778	leh	57.3896	-91.797	37
	BC	57.3893	-91.7973	37.5
PRAD121-780	leh	57.4059	-91.7288	49
	BC	57.407	-91.7272	48

### 3.2. Physical analyses

The whole cores were first scanned with a GEOTEK XCT digital X-ray system at ISMER to obtain digital X-ray images of the cores which were then displayed with grey-scale values. Subsequently, the cores were analyzed with a GEOTEK Multi Sensor Core Logger (MSCL) to measure wet bulk density by gamma ray ( $\gamma$ ) attenuation and low-field volumetric magnetic susceptibility ( $k_{LF}$ ) at 0.5 cm intervals. This last parameter is sensitive to ferrimagnetic mineral concentration and grain size variations (e.g., St-Onge et al., 2007).

Using these first results the best preserved push-core for each site (best apparent sediment/water interface, no coring artefact and no compaction) was selected and opened, along with all the gravity cores. Once split, the cores were described and analyzed one more time with the MSCL to measure diffuse spectral reflectance parameters ( $L^*$  presented for core 772) using a Minolta spectrophotometer, magnetic susceptibility using a Bartington point sensor, and elemental composition and concentration with a Innov-X X-ray fluorescence (XRF) spectrometer at 0.5 cm intervals. Elemental ratios obtained by

XRF data provide information about sediment characteristics and associated processes: a good example is the Zr/Rb ratio that allows identifying turbidites (Croudace et al., 2006).

Finally, the split cores were sampled with u-channels (u-shaped plastic liner of 2x2 cm cross-section and up to 1.5 m in length) for rock-magnetic analyses. Shells were collected for  $^{14}\text{C}$  dating, and discrete samples were taken for grain-size, rock-magnetic and geochemical analyses.

### *3.3. Grain-size analyses*

The sediment grain-size is one of the main indicators of hydrodynamic changes through time. For grain-size measurements, discrete samples were collected at 4 cm intervals from the gravity cores, diluted into a Calgon solution (1% sodium hexametaphosphate) and mixed several hours using a house-made rotator before analysis. These analyses were performed using a Beckman Coulter LS13320 laser sizer and the results were computed with GRADISTAT to determine grain-size statistical data (Blott & Pye, 2001).

### *3.4. Magnetic analyses*

The magnetic properties of sediments can be used in several ways. The rock-magnetic properties, which are inherent to the sediment composition, enable detection of variations in grain size, concentration and mineralogy of magnetic minerals, which are influenced by environmental changes (Tauxe, 2010; Liu et al., 2012). For example, the  $k_{\text{ARM}}/k$  ratio is inversely correlated to grain-size variations if magnetite dominates the magnetic signal (e.g. Stoner et al., 1996; Liu et al., 2012).

The u-channels sampled in the cores were analyzed with a 2G SRM-755 u-channel cryogenic magnetometer to measure ARM by inducing an alternating field of 100 mT with a 0.05 mT direct current (DC) biasing field. The ARM was then normalized by the biasing field used to obtain  $k_{\text{ARM}}$ , which is used in the  $k_{\text{ARM}}/k_{\text{LF}}$  ratio (King et al., 1983). In addition, an alternating gradient force magnetometer (AGM) was used on discrete samples to measure hysteresis properties of the sediment; saturation magnetization ( $M_s$ ), coercive force ( $H_c$ ), saturation remanence ( $M_{\text{rs}}$ ), and coercivity of

remanence ( $H_{cr}$ ). The resulting hysteresis curve is indicative of the magnetic mineralogy and grain-size (Tauxe et al., 1996) and is useful to determine if magnetite is the dominant magnetic mineralogy, and thus the validity of the  $k_{ARM}/k_{LF}$  ratio to reflect changes in grain-size.

### *3.5. Chemical analyses*

A minor fraction of marine and lacustrine sediment is composed by organic matter that is the residue of past biota. The composition and the amount of this matter reflect changes in environmental conditions in the past (Meyers, 1997). For example, isotopic ratios such as  $\delta^{13}\text{C}$  and  $\delta^{15}\text{N}$ , together with the elemental ratio C/N, allow identification of variations in the sediment source between marine algae, lacustrine algae or terrestrial plants (e.g., Meyers, 1997; St-Onge and Hillaire-Marcel, 2001). In this study, samples from core 772 were collected at the same interval as for grain-size analyses (every 4 cm) and then split in two subsamples. They were dried and crushed, and one of the two subsamples was treated with HCl to remove inorganic carbon. All samples were then analyzed with a gas chromatograph coupled to a mass spectrometer for stable isotope ( $\delta^{13}\text{C}$ ) and an elemental analyzer (GC-EA-IRMS, ThermoElectron/COSTECH) to measure C and N contents (%C, %N). By combining the data from the treated and untreated samples, we can then determine  $C_{total}$ ,  $N_{total}$ ,  $C_{inorg}$  and  $C_{org}$ , and the C/N elemental ratio.

### *3.6. Chronology*

In total, 20 mollusk shells were collected from the four gravity cores and from one of the box cores for radiocarbon dating (Table 2), and were sent to the Radiochronology Laboratory at Université Laval for pre-treatment. The  $^{14}\text{C}$  ages were then determined at the W. M. Keck Carbon Cycle Accelerator Mass Spectrometer Laboratory at the University of California, Irvine, USA. The resulting  $^{14}\text{C}$  ages were calibrated by using the CALIB 7.0 online calibration software (Stuiver et al., 2005) and the MARINE13 dataset (Reimer et al., 2013). A marine reservoir correction ( $\Delta R$ ) of 110  $\pm$  65 years, recognized for Hudson Bay (Coulthard et al., 2010), was applied and the calibrated ages are reported with the  $2\sigma$  confidence level.

Recent sedimentation rates for all the sites were derived using the  $^{210}\text{Pb}$  activity of dried and crushed sediments determined by alpha spectrometry of the daughter isotope  $^{210}\text{Po}$  at the GEOTOP research center (Zhang, 2000). The sedimentation rate (SR) is obtained through the slope of a linear regression between the  $\ln(^{210}\text{Pb}_{\text{excess}})$ , which was calculated by subtracting the supported  $^{210}\text{Pb}$  determined visually on the activity versus depth graph. For these analyses, sediment was sampled from the selected box cores at each centimeter from 0 to 20 cm and each 5 cm on the rest of the cores.

**Table 2.** AMS  $^{14}\text{C}$  dated material and results.

Core	Depth (cm)	Dated material	Lab number	University of California	Conventional $^{14}\text{C}$ age (yr BP)	Calibrated age <sup>a</sup> (ca BP)
PRAD121-772-leh	125	Unidentified shell fragments	ULA-4128	UCIAMS-125601	1975 ± 15	1279 (1415) 1552
PRAD121-776-BC-B	20	Barnacle	ULA-4385	UCIAMS-132536	Modern	
PRAD121-776-leh	71	Barnacle	ULA-4129	UCIAMS-125602	640 ± 15	0 (157) 272
		<i>Macoma</i> sp	ULA-4130	UCIAMS-125603	915 ± 15	297 (434) 528
		Unidentified shell fragment	ULA-4131	UCIAMS-125604	880 ± 15	283 (403) 505
PRAD121-778-leh	39	Unidentified shell fragment	ULA-4375	UCIAMS-132528	Modern	
	53	<i>Admete Couthoni</i>	ULA-4374	UCIAMS-132527	605 ± 15	0 (125) 251
	66	<i>Macoma</i> sp	ULA-4373	UCIAMS-132526	920 ± 15	298 (439) 532
	140	Unidentified shell fragment	ULA-4132	UCIAMS-125605	990 ± 20	369 (498) 628
	147	<i>Eumicula</i> sp	ULA-4372	UCIAMS-132525	1280 ± 20	618 (724) 885
	214	<i>Macoma</i> sp	ULA-4133	UCIAMS-125606	975 ± 15	355 (486) 614
PRAD121-780-leh	81	<i>Veneridae</i> sp	ULA-4376	UCIAMS-132531	Modern	
	106	<i>Macoma</i> sp	ULA-4134	UCIAMS-125607	1040 ± 15	443 (539) 645
	125	Unidentified shell fragment	ULA-4135	UCIAMS-125608	1205 ± 15	534 (656) 775
	139	Barnacle	ULA-4136	UCIAMS-125609	965 ± 15	328 (478) 599
	140	<i>Macoma</i> sp	ULA-4377	UCIAMS-132532	1065 ± 15	464 (537) 654
	187	Unidentified shell fragment	ULA-4378	UCIAMS-132533	850 ± 15	269 (380) 492
	216	Unidentified shell fragment	ULA-4137	UCIAMS-125610	885 ± 15	285 (408) 507
	230	Barnacle	ULA-4138	UCIAMS-125611	835 ± 15	259 (369) 488
	241	<i>Cerastoderma Pinnulatum</i>	ULA-4379	UCIAMS-132534	660 ± 15	0 (174) 290

<sup>a</sup> The first and last ages represent the  $2\sigma$  cal age range, whereas the ages in parentheses are the average age. The calibration includes a marine reservoir correction of  $110 \pm 65$  yr proposed by Coulthard et al. (2010) for Hudson Bay.

## 4. Results

### 4.1. Core top correlation

Comparison between the gravity cores and their respective box cores was performed using the MSCL parameters (Fig. 5). Cores 772 and 776 did not reveal any missing sediment at the top of the gravity cores. However, the gravity cores of sites 778 and 780 show 7 and 25 cm of missing sediments respectively.

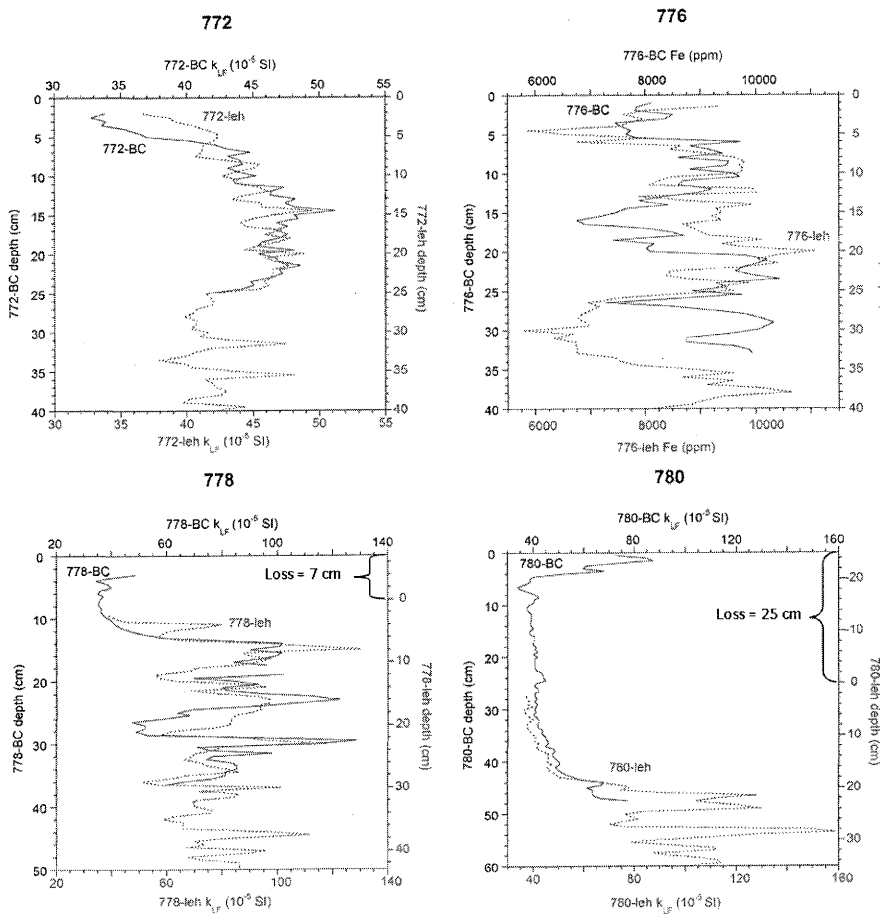


**Figure 5.** Correlation (magnetic susceptibility  $k_{LF}$  or Fe content) between the *LeHigh* gravity core (leh; in red) and the box-core (BC; in black) for the four sites sampled. Even though the Fe results are presented as ppm, only relative changes were used here as an absolute calibration with sediments was not performed.

#### 4.2. Lithology

##### 4.2.1. Core 772

Core 772 is mainly composed of fine silt around  $11 \mu\text{m}$  (Fig. 6). The homogenous nature of the core is also illustrated by the physical, chemical and magnetic properties of the sediment which only show minor variations with the depth. The magnetic susceptibility and the  $k_{ARM}/k$  ratio increase slightly from bottom to top, mostly between 50 and 0 cm, whereas density, mean grain size and the Zr/Rb ratio are relatively constant.  $L^*$  decreases somewhat from 50 cm to the top, according to the darker color of the sediment that was visible on the opened core. The organic carbon content increases slightly from 0.3% at the base to 0.6% at the top of the core, and the  $\delta^{13}\text{C}$  only shows an increasing trend in the upper 20 cm. The C/N ratio does not show any significant trend.

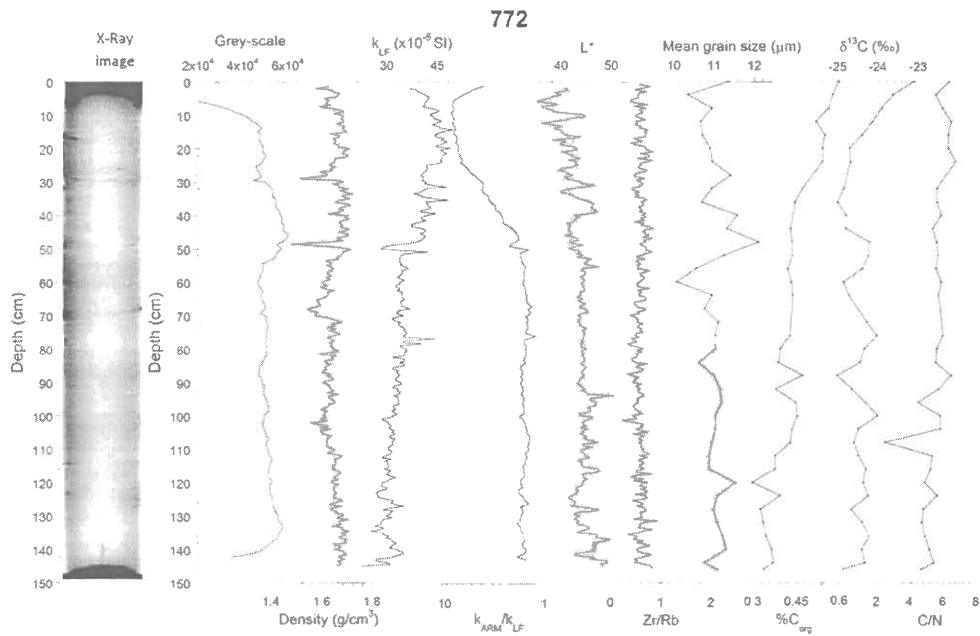


**Figure 6.** X-Ray image and derived grey scale values, physical, sedimentological, magnetic and geochemical properties of core 772 versus depth.

#### 4.2.2. Core 776 (Churchill River)

Similarly to core 772, core 776 does not show large lithological variations. It is mainly composed of medium silt, generally coarser than the sediments of core 772 (Fig. 7), and contains a few gravel particles (< 1.5 cm in diameter) scattered in the core. At 51 cm, there is a sharp and thin layer of fine sand underlying a laminated interval of finer material composed of fine silt. These variations are mirrored by the mean grain-size, as well the  $k_{ARM}/k$  and Zr/Rb ratios. The upper part of the core (0-20 cm) is slightly coarser than the rest, but this is not observed in the  $k_{ARM}/k$  and Zr/Rb ratios.

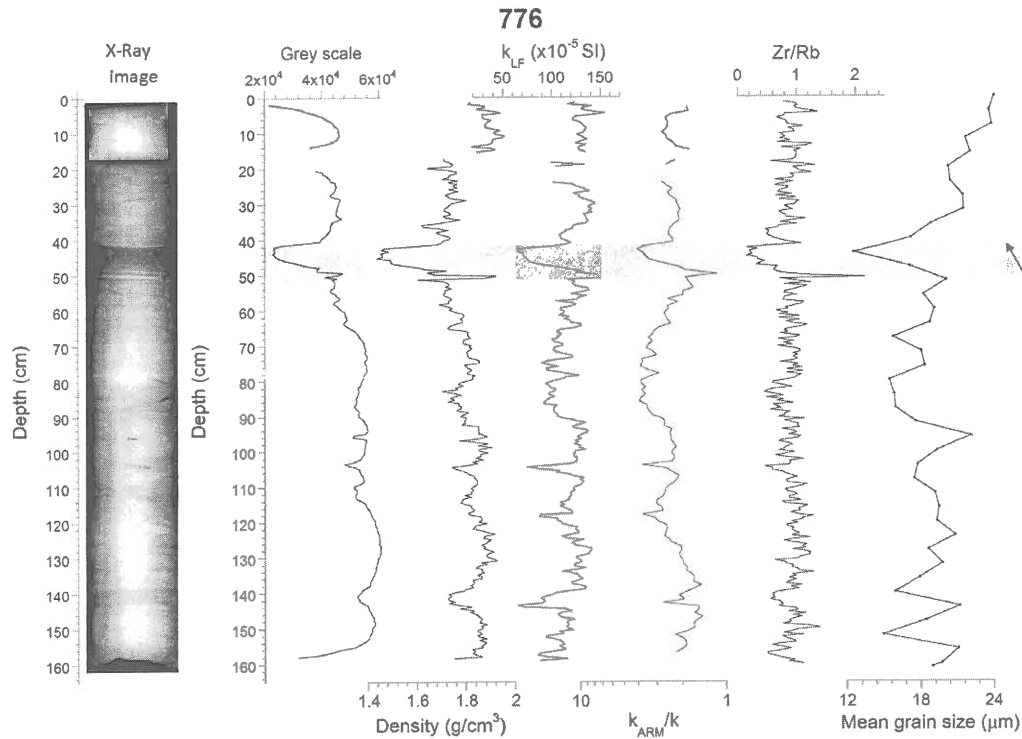


**Figure 7.** X-Ray image and derived grey scale value, physical, sedimentological, magnetic and geochemical properties of core 776 versus depth.

#### 4.2.3. Cores 778 and 780 (*Nelson River*)

As shown by the X-ray images, cores 778 and 780 depict larger lithological variations than the other cores with a composition varying between clay and fine sand (Fig. 8). The grey scale values, wet-bulk density and grain-size data indicate a similar pattern for the two cores with a lower part characterized by gradual alternations between coarser and finer layers, and an upper part with higher frequency variations (Fig. 8). The layers of the lower part of both cores are characterized by a coarsening upward unit followed by a fining upward unit: these variations are highlighted by the  $k_{ARM}/k$  and Zr/Rb ratios, which are influenced by grain-size variations (Croudace et al., 2006; Liu et al., 2012). Cores 778 and 780 contain, respectively, 12 and 11 of these layers, identified as rapidly deposited layers (RDLs). The coarsening upward layers often contain gravel particles usually smaller than 5 mm, and the fining upward layers are often laminated. The transition from the coarsening to the fining layer is generally gradual but sometimes sharp, as in RDL 9 and 10 in core 780. Using their size, the shape of the different parameters, and the interval between them, it is possible to recognize the same RDL from a core to another (Fig. 9). In the upper part of the cores (0-60 cm in 778, and 0-90 cm in 780), the variations become thinner and single events are difficult to distinguish.

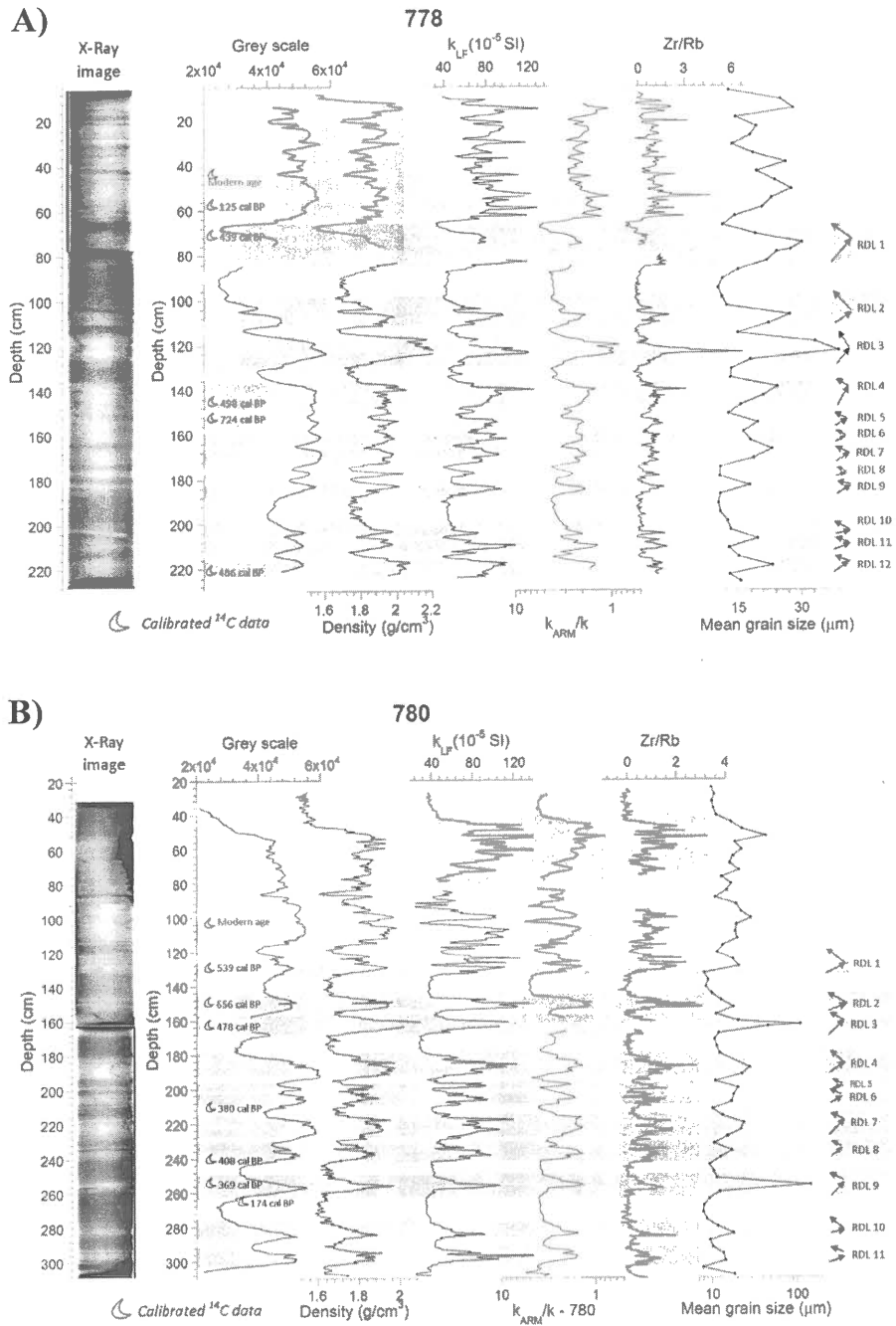


**Figure 8.** X-Ray image and derived grey scale value, physical, sedimentological, magnetic and geochemical properties versus depth for the gravity cores of sites A) 778 and B) 780, with the non-corrected depths. The  $^{14}\text{C}$  ages are indicated. The RDL are highlighted in grey and the upper part in yellow.

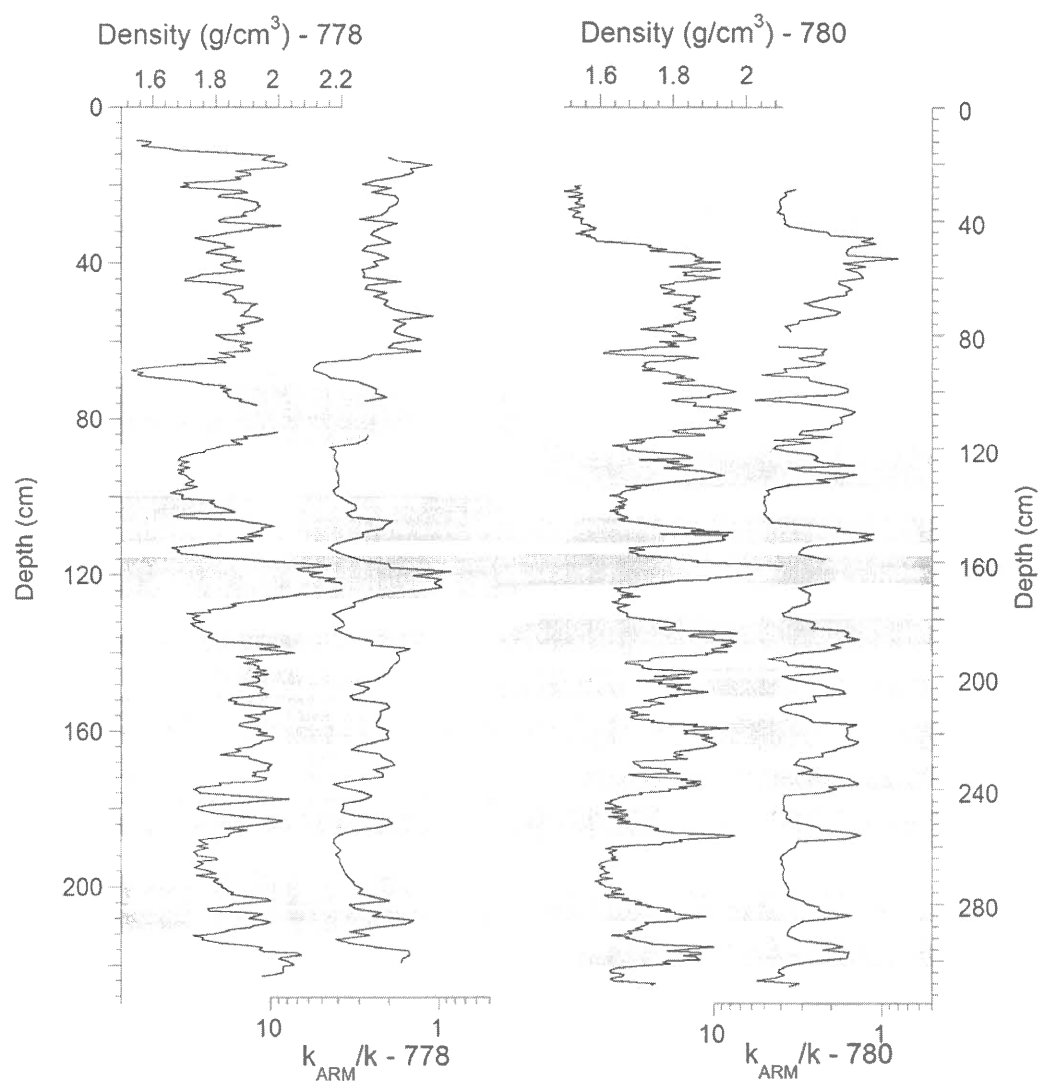


**Figure 9.** Comparison between cores 778 and 780 with the density and the  $k_{\text{ARM}}/k$  ratio after depth correction to account for the missing sediment in the upper part of the cores. The RDL are highlighted in grey, whereas the upper variations are in yellow.

### 4.3. Rock-magnetic data

The hysteresis curves obtained on selected samples from the cores yielded indications on the mineralogy and grain-size of the magnetic grains present in the sediment (Tauxe et al., 1996). All curves have the typical shape of the predominance of low-coercivity minerals such as magnetite (Fig. 10), and this indicates that the  $k_{ARM}/k$  ratio can be used as a grain-size indicator (Liu et al., 2012). The difference between the two samples of core 780 highlights the contrast between their grain sizes (Fig. 10 D and E). The sample D, collected from the background sediments, has a higher value of coercivity due to the finer grains of magnetite, whereas the sample E, from a RDL peak, illustrates the presence of coarser magnetite grains (Tauxe et al., 1996).

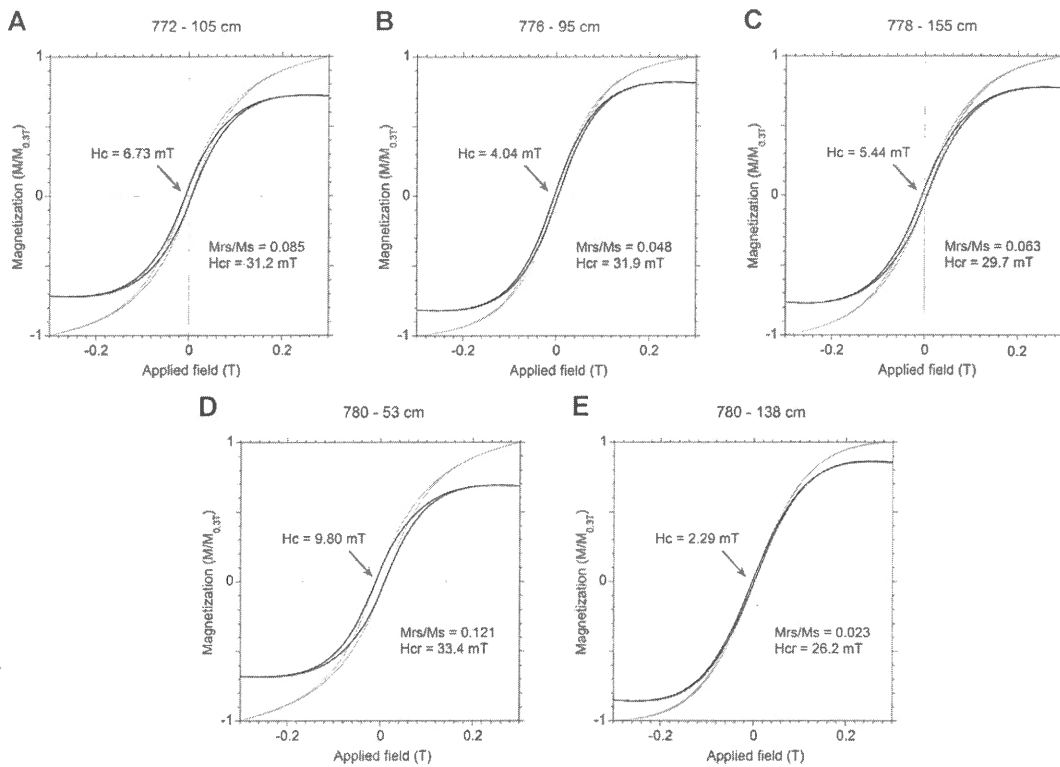


**Figure 10.** Hysteresis curves and derived parameters of a representative sample from each core 772 (A), 776 (B) and 778 (C), and 2 samples from core 780 (D and E). In D), the sample is from finer background sediments, while in E) it is from a coarser RDL.

#### 4.4. Chronology

##### 4.4.1. Core 772

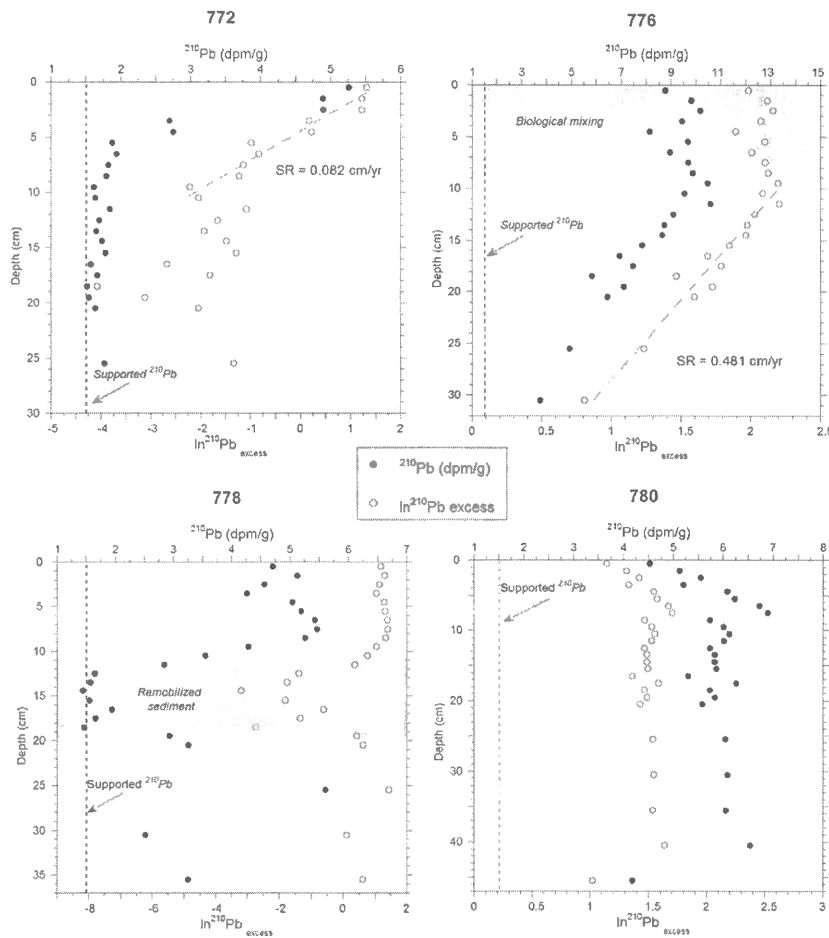


**Figure 11.**  $^{210}\text{Pb}$  measurements for the four cores with the derived sedimentation rate (SR). Biological mixing occurs in cores 776, 778 and 780. The regional supported  $^{210}\text{Pb}$  is determined by the trend of  $^{210}\text{Pb}$  in core 772.

Several shell fragments were found in core 772 (at 125 cm depth) and were dated to 1415 cal BP (Table 1).  $^{210}\text{Pb}$  activity determined on core 772 is characterized by a clear exponential decrease, corresponding to a sedimentation rate of 0.082 cm/yr at the top of the core (Fig. 11), which is closed to the value of ~0.09 cm/yr obtained by Kuzyk et al. (2009)

on a nearby core. Together, the  $^{14}\text{C}$  age and the  $^{210}\text{Pb}$  activity data indicate that core 772 spans the past 1800 years (Fig. 12).

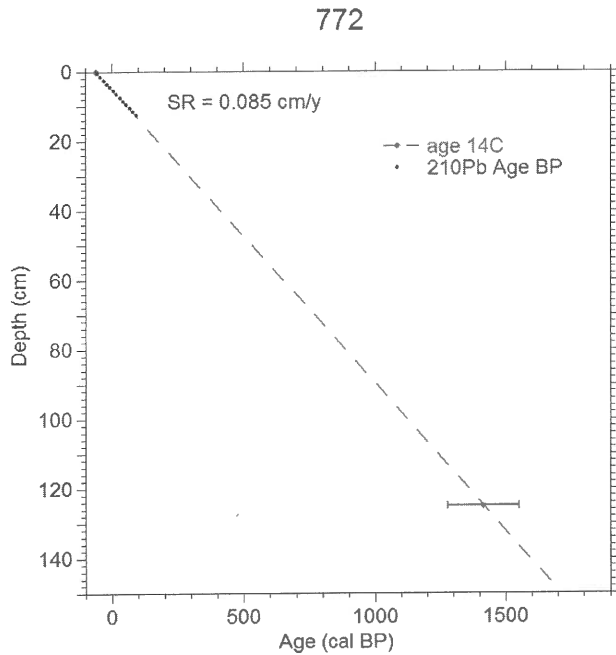


**Figure 12.** Age-model of core 772 based on the  $^{14}\text{C}$  age and  $^{210}\text{Pb}$  data.

#### 4.4.2. Core 776

For site 776, there is a clear decrease of  $^{210}\text{Pb}$  activity between 9 and 31 cm, whereas the upper 9 cm are constant and probably reflect biological mixing (Fig. 11). The resulting sedimentation rate is  $\sim 0.48 \text{ cm/yr}$ , which is coherent with the  $^{14}\text{C}$  ages obtained for this core (Table 1). In addition, since the regional supported value is not reached in this core, sedimentation rates could be higher. The result is that this core spans the last 350 years, and possibly less.

#### 4.4.3. Cores 778 and 780

For cores 778 and 780, most of the  $^{14}\text{C}$  ages are reversed, i.e. younger ages were found deeper in the cores (Table 2). Moreover,  $^{210}\text{Pb}$  activity does not show a clear decrease in both cores, despite the shift between 10 and 19 cm in core 778 (Fig. 11). Therefore, it was not possible to establish a chronology for these cores. However, modern ages were found in the upper part of the cores; at 35 cm in core 778, and at 81 cm in core 780, suggesting that recent sedimentation rates are relatively high. Such high rates, or an intense biological mixing, could explain why the sediment in box-cores 778 and 780 does not show a  $^{210}\text{Pb}$  activity decrease.

## 5. Discussion

### 5.1. Environmental changes since the last 1800 years

The relatively homogeneous nature of core 772 illustrates that the sedimentation dynamics at this site have not been highly influenced by the climatic variations of the last 1800 years, nor by hyperpycnal flows as no rapidly deposited layers were observed in this core. The core location, farther from the coast than the others, explains the lack of notable variations. This area is less influenced by coastal processes and the sedimentation rate is lower than in coastal areas due to its more distal position. The notable decrease of organic carbon content and the increase of the L\* value indicate a higher organic matter content in the uppermost 20 cm. This higher content can be related to organic matter degradation downcore and/or a recent increase in marine production as indicated by the increase in  $\delta^{13}\text{C}$  values (Meyers, 1997). This change might be explained by the increasing duration of the ice-free season in south-western Hudson Bay in the last decades (Gough et al., 2004; Gagnon & Gough, 2005).

### 5.2. Rapidly deposited layers

The RDLs of cores 778 and 780 are identified as hyperpycnites; a type of deposit formed by a turbulent flow carrying a high load of particles making its density higher than the ambient density of the standing water-body, i.e. a hyperpycnal flow (e.g.: Mulder and Syvitski, 1995; Mulder et al., 2003). These flows mainly occur during river floods caused by seasonal and/or catastrophic events, and the resulting hyperpycnite contains a reverse graded unit deposited during the waxing phase of the flood, and a normal graded unit deposited during the waning phase of the flood (e.g., Mulder et al., 2003; St-Onge et al., 2004). Such floods in cold regions can occur during spring ice-breaking, especially with the formation of ice-jams (Prowse, 1994; Beltaos, 2007). In this case, the sediment concentration can highly increase due to the increasing river flow, the higher water level, and the eroding effect of ice on the river bed and reaches (Prowse, 1993).

The Nelson River is not included in the “dirty rivers” identified by Mulder and Syvitski (1995) which are rivers able to often generate hyperpycnal flows. However, Mulder and Chapron (2010) suggested that 71% of rivers discharging into the world oceans may generate a hyperpycnal flow every 1 to 100 years, exclusively during floods, depending on how clean they are. This percentage increases to 84% if we take into account the convective instability at river mouths (Parsons et al., 2001). Great rivers with a large drainage basin are not normally supposed to generate hyperpycnal flows due to the dilution of the sediment load and the existence of different climatic conditions over the basin (Mulder and Syvitski, 1995; Mulder and Chapron, 2010). However, before the construction of hydroelectric dams, the lower Nelson River had a 250 km long ice-cover each winter (Rosenberg et al., 2005) that could form ice jam during the freezing or the breaking (Fig. 13 A; e.g., Prowse, 1994; Jeffries et al., 2012). The breaking of ice-jams are more common if the seasonal advance of snowmelt runoff proceeds in a downstream direction (Prowse, 1994), which is the case of the Nelson River, flowing north-east. At the time of a major ice-jam failure, floods were generated by the retained waters. The erosion was accentuated by the floods, increasing the sediment concentration in the flowing water and, thus, this water became sufficiently dense to produce a hyperpycnal flow downstream (Fig. 13 B). Each hyperpycnite recorded in cores 778 and 780 (Fig. 8) therefore most likely represents one important hyperpycnal flow of the Nelson River triggered by the breaking of a major ice-jam (Fig 13 A and B). The cores probably do not contain the signature of all the floods of this river, but only the floods that can both create hyperpycnal flows and bring sediments at the core sites.

In the case of core 776, only one layer was identified as a RDL. However, it does not contain a visible inverse-graded layer. This normal-graded layer could be a Bouma-like turbidite, but the fine sand at the base of the RDL suggests that it could be a hyperpycnite deposited by a high-magnitude hyperpycnal flow, which has eroded the waxing-phase layer (Mulder et al., 2003). The lack of other RDLs may be due to the distal location of the coring site and to the shape of the Churchill River estuary, which is enclosed and has a weir located at the upstream end (Kuzyk et al., 2008), unlike the open estuary of the Nelson

River mouth. The lower discharge of the Churchill River compared to Nelson River (1350 vs 2240 m<sup>3</sup>/s, before dams) could also play a role in explaining why hyperpycnal flows did not reach the sampling site.

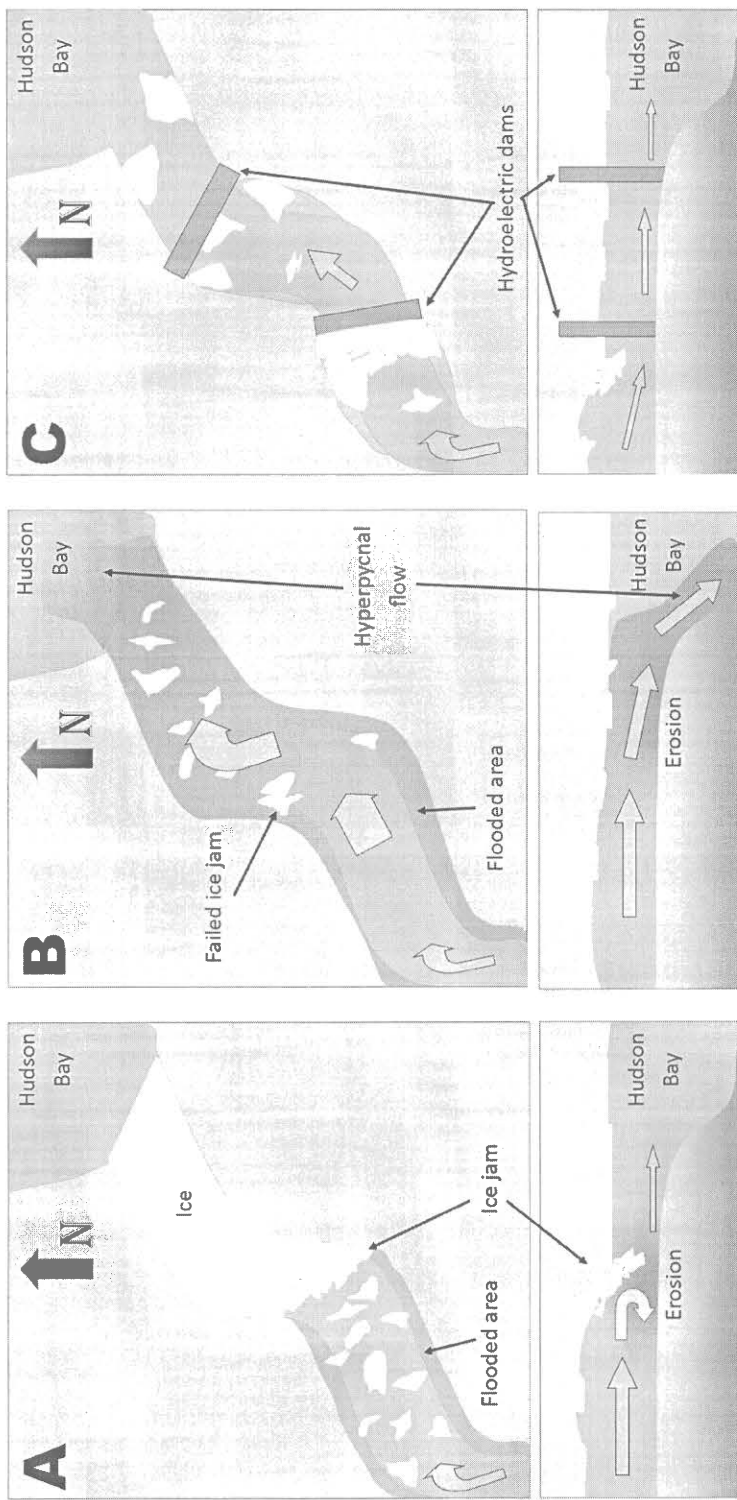


**Figure 13.** Representation of a river with A) an ice-jam, B) a subsequent hyperpycnal flow and C) hydroelectric dams that prevent the floods.

### *5.3. Impact of river damming on the Nelson River dynamics*

Even if a precise chronology cannot be established, it is possible to reach some conclusion. Firstly, most of the pelecypod shells used for  $^{14}\text{C}$  dating were sampled in the coarser part of the different hyperpycnites (Fig 8), suggesting that they were remobilized during the peaks of hyperpycnal flows. Only one shell, located at 241 cm in core 780, seems to be in-situ, and has been dated at 174 cal BP. This age suggests a sedimentation rate of about 1 cm/yr, but this value is biased by the hyperpycnite layers that are assumed to be deposited almost instantaneously (St-Onge et al., 2012). However, all the identified hyperpycnites are situated below a specific depth in cores 778 and 780, above which the variations are much thinner. This contrast suggests a major change in the sedimentary regime, and thereby also in the Nelson River hydrodynamics. The presence of modern  $^{14}\text{C}$  ages at a depth of 39 cm in core 778 and 81 cm in core 780 implies that this major change happened around 1950 AD, coinciding with the important anthropogenic modifications of the area, i.e., hydroelectric dams and the Churchill River diversion (Newbury et al., 1984; Anctil & Couture, 1994; Rosenberg et al., 2005). The hydroelectric dams built on the Nelson and Churchill Rivers allow a continuous control of their flow, causing a regulation of their hydrograph (Anctil & Couture, 1994), and preventing the progressive natural river icing and damming (Rosenberg et al., 2005). Moreover, the control of the river flow prevents high discharge that might trigger ice-jam flooding downstream and the formation of hyperpycnal flows (Beltaos, 1995; Jeffries et al., 2012). These anthropogenic controls of river hydrology are thereby a possible explanation for the absence of relatively thick hyperpycnites in the upper/younger parts of cores 778 and 780. The high-frequency variations observed in these upper parts may be due to small ice-jams that can still occur downstream the Limestone Generating station (North/South Consultants Inc., 2012). It also might be caused by sediment flushing or sluicing that are used to increase the lifetime of reservoirs with high sedimentation rates (Brandt, 2000).

## 6. Conclusions

The physical, chemical and magnetic properties of sediment cores sampled near the Churchill and Nelson River mouths allowed identification of the impact of river damming on the flow and sediment dynamics of these rivers. The dam construction on the Nelson River in the 1960s changed the sediment dynamics downstream by preventing the formation of major ice-jams. Prior to this installation, major ice-jamming often occurred on the lower Nelson River during the ice break-up and spring freshet. The breaching of such ice jams triggered river floods and increased erosion of the reaches, allowing the formation of hyperpycnal floods. The signature of these floods can be recognized in the lower parts of cores 778 and 780, both sampled near the Nelson River mouth: they contain rapidly deposited layers identified as hyperpycnites. The upper parts, however, do not show such structures. Despite the lack of precise chronology, modern  $^{14}\text{C}$  ages in both cores suggest that the transition towards the upper part of the cores is concurrent with the dam construction on the Nelson River. The dams allow a control of the floods and reduce the downstream transport of ice, preventing major ice-jam formation and hyperpycnal flows. The Churchill River ends in an enclosed estuary that may reduce the offshore impact of floods and could explain the absence of more than one hyperpycnite in core 776, which also covers a shorter time period than the other cores. Finally, core 772, sampled 200 km offshore, is relatively homogenous and is used as a reference core without major river influence. To obtain a longer record of past flood events, new cores could be sampled directly in the river mouth, especially in the enclosed estuary of the Churchill River.

## CONCLUSION GÉNÉRALE

Ce projet de maîtrise a permis d'identifier l'influence de facteurs anthropiques sur l'écoulement d'importantes rivières de l'ouest de la baie d'Hudson dans la 2<sup>ème</sup> moitié du 20<sup>ème</sup> siècle. Il s'avère que, avant la construction des barrages sur le fleuve Nelson, les processus naturels contrôlaient son débit. Ainsi, lors des périodes de débâcle, la partie inférieure du fleuve était souvent sujette à la formation d'embâcles majeurs qui causaient d'importantes crues. Par la suite, la construction de barrages sur le fleuve Nelson dans les années 1960 a permis d'empêcher la formation de tels embâcles et d'éviter ces crues majeures, modifiant ainsi la dynamique du transport sédimentaire jusqu'à l'embouchure.

Tout cela a été déterminé par la présence de couches sédimentaires particulières dans les carottes échantillonnées à l'embouchure du fleuve Nelson (778 et 780) et absentes dans la carotte de référence prise au large (772). Ces couches déposées rapidement, identifiées par les diverses analyses de paramètres physiques, de propriétés magnétiques, sédimentologiques et de la composition chimique du sédiment, présentent les caractéristiques des hyperpycnites. Ces couches sont notamment caractérisées par un granoclassement inverse suivi d'un granoclassement normal qui traduit une accélération puis une décélération de la vitesse de l'écoulement. Ce sont des crues à forte charge sédimentaire, causées par la rupture d'embâcles qui bloquaient les eaux, qui auraient formé des courants hyperpycnaux à l'embouchure et permettant ainsi le dépôt des hyperpycnites. Ces couches sont absentes des sections supérieures de ces carottes, qui montrent des variations moins marquées ne permettant pas l'identification de couches déposées rapidement.

La chronologie fut complexe à établir en raison de la présence de nombreuses inversions dans les âges <sup>14</sup>C. En effet, des âges plus anciens ont été retrouvés plus haut dans la carotte, mais tous au sein de couches déposées rapidement, ce qui indique que le matériel daté dans ces intervalles a probablement été remobilisé par les courants hyperpycnaux. De même, les mesures de <sup>210</sup>Pb effectuées sur des sédiments en partie remobilisés ne

permettent pas d'établir avec précision les vitesses de sédimentation pour ces carottes. Cependant, ces mesures ainsi qu'un âge  $^{14}\text{C}$  obtenu sur une coquille trouvée en position de vie permettent d'affirmer que la vitesse de sédimentation est particulièrement élevée, de l'ordre de 1 cm/an voir plus, et que les carottes 778 et 780 couvrent environ 300 ans. De plus, des âges  $^{14}\text{C}$  modernes obtenus près de la transition entre les sédiments avec et sans hyperpycnites indiqueraient que ce changement de dynamique sédimentaire serait dû à l'aménagement du fleuve par la construction des barrages hydroélectriques. Ces barrages segmentent le fleuve, permettent de contrôler son débit et réduisent le transport de glace vers l'aval, empêchant ainsi la formation d'embâcles majeurs, et donc de courants hyperpycnaux. Les variations observées dans les parties supérieures des carottes peuvent s'expliquer par l'impact d'embâcles mineurs sur les 80 km qui séparent le dernier barrage (station Limestone) et l'embouchure du fleuve. D'autre part, la vidange des réservoirs, où le sédiment s'accumule, peut aussi entraîner une quantité notable de matière en aval et expliquer ces variations.

De son côté, la carotte 776 échantillonnée près de la rivière Churchill a révélé ne contenir qu'une seule hyperpycnite. En plus du fait qu'elle ne couvre que 350 ans environ, des facteurs géomorphologiques et hydrologiques ont été proposés afin d'expliquer l'absence de plusieurs hyperpycnites dans cette carotte. Une meilleure étude de la région pourrait aider à mieux comprendre les processus à l'origine de cette différence de dynamique entre les deux rivières. Par ailleurs, il serait judicieux d'échantillonner des carottes plus longues directement à l'embouchure des deux cours d'eau et dans l'estuaire fermé de la rivière Churchill dans le but d'obtenir des enregistrements plus complets des événements de crues au cours des derniers millénaires. De plus, considérant les fortes vitesses de sédimentation des carottes 778 et 780, il serait possible de réaliser d'autres mesures de  $^{210}\text{Pb}$  sur des sections plus en profondeur et non remobilisées afin d'obtenir une meilleure précision et de pouvoir établir une corrélation entre la fréquence des hyperpycnites et les facteurs climatiques tels que l'ENSO et la PDO.

Finalement, ce mémoire de maîtrise montre qu'une étude multi-paramètres peut être grandement bénéfique pour étudier la dynamique des rivières. Par exemple, les ratios  $k_{ARM}/k$  et Zr/Rb déterminés à haute résolution (1 cm) sont tous sensibles aux variations de granulométrie mais, chaque paramètre pouvant être influencé par d'autres facteurs que la granulométrie (e.g., minéralogie), leur combinaison avec des analyses sédimentologiques plus classiques (granulométrie) réalisées à plus faible résolution (4 cm) permet de confirmer les interprétations faites sur les mesures à plus haute résolution et ainsi bénéficier d'une précision maximale.

## RÉFÉRENCES BIBLIOGRAPHIQUES

- Anctil, F., Couture, R., 1994. Impacts cumulatifs du développement hydro-électrique sur le bilan d'eau douce de la baie d'Hudson. *Canadian Journal of Civil Engineering*, **21**, 297-306.
- Barber, D. C., Dyke, A., Hillaire-Marcel, C., Jennings, A. E., Andrews, J. T., Kerwin, M. W., Bilodeau, G., McNeely, R., Southons, J., Morehead, M. D., Gagnon, J.M., 1999. Forcing of the cold event of 8,200 years ago by catastrophic drainage of Laurentide lakes. *Nature* **400**, 344–348.
- Beltaos, S. (Editor). 1995. River ice jams. Water Resources Publications, LLC, Colorado. 372 p
- Beltaos, S., Prowse, T. D., 2001. Climate impacts on extreme ice-jam events in Canadian rivers. *Hydrological Sciences*, **46**:1, 157-181.
- Beltaos, S., Burrell, B. C., 2003. Climatic change and river ice breakup. *Canadian Journal of Civil Engineering*, **30**, 145-155.
- Beltaos, S., 2007. River ice breakup processes: recent advances and future directions. *Canadian Journal of Civil Engineering*, **34**, 703-716.
- Blott, S.J., Pye, K., 2001. Gradistat: a grain size distribution and statistics package for the analysis of unconsolidated sediments. *Earth Surface Processes and Landforms* **26**, 1237–1248.
- Bodaly, R. A., Hecky, R. E., Fudge, R. J. P., 1984. Increases in Fish Mercury Levels in Lakes Flooded by the Churchill River Diversion, Northern Manitoba. *Canadian Journal of Fisheries and Aquatic Sciences*, **41**, 682-691.
- Bonsal, B., Shabbar, A. 2011. Oscillations climatiques à grande échelle ayant une incidence sur le Canada, de 1900 à 2008. Biodiversité canadienne : état et tendances des écosystèmes en 2010, Rapport technique thématique no4. Conseils canadiens des ministres des ressources.Ottawa, ON. iii + 15 p.
- Boyer-Villemaire, U., St-Onge, G., Bernatchez, P., Lajeunesse, P., Labrie, J., 2013. High-resolution multiproxy records of sedimentological changes induced by dams in the Sept-Îles area (Gulf of St. Lawrence, Canada). *Marine Geology*, **338**, 17-29.
- Brandt, S. A., 2000. Classification of geomorphological effects downstream of dams. *Catena*, **40**, 375-401.
- Burn, D.H., 1994. Hydrologic effects of climatic change in west-central Canada. *Journal of Hydrology* **160**, 53–70.

- Coulthard, R. D., Furze, M. F. A., Piénkowski, A. J., Nixon, F. C., England, J. H., 2010. New marine  $\square$ R values for Arctic Canada. *Quaternary Geochronology*, **5**, 419-434.
- Croudace, I. W., Rindby, A., Rothwell, R. G., 2006. ITRAX: description and evaluation of a new multi-function X-ray core scanner. From: Rothwell, R.G. 2006. New Techniques in Sediment Core Analysis. *Geological Society of London, Special Publications*, **267**, 51-63.
- Déry, S. J., Wood, E. F., 2005. Decreasing river discharge in northern Canada. *Geophysical Research Letters*. vol. **32**, L10401.
- Déry, S. J., Stieglitz, M., McKenna, E. C., Wood, E. F., 2005. Characteristics and trends of river discharge into Hudson, James and Ungava Bays, 1964-2000. *Journal of climate*, **18**, 2540-2557.
- Déry, S. J., Mlynowski, T. J., Hernández-Henríquez, M. A., Straneo, F., 2011. Interannual variability and interdecadal trends in Hudson Bay streamflow. *Journal of Marine Systems* **88**, 341-351.
- Dyke, A.S., 2004. An outline of North American deglaciation with emphasis on central and northern Canada. In: Ehlers, J., Gibbard, P.L. (Eds.), *Quaternary Glaciations—Extent and Chronology, Part II: North America*, pp. 373–424.
- Gagnon, A. S., Gough, W. A., 2005. Trends in the dates of ice freeze-up and breakup over Hudson Bay, Canada. *Arctic*, **58**, 4, 370-382.
- Gough, W. A., Cornwell, A. R., Tsuji, L. J. S., 2004. Trends in Seasonal Sea Ice Duration in Southwestern Hudson Bay. *Arctic*, **57**, 3, 299-305.
- Jeffries, M. O., Morris, K., Duguay, C. R., 2012. Floating ice: Lake ice and river ice. *Satellite Image Atlas of Glaciers of the World. Vol.A: State of the Earth's Cryosphere at the Beginning of the 21st Century: Glaciers, Global Snow Cover, Floating Ice, and Permafrost and Periglacial Environments*. U.S. Geological Survey Professional Paper 1386-A, A381–A424.
- Kirk, J. L., St-Louis, V. L., 2009. Multiyear total and methyl mercury exports from two major sub-arctic rivers draining into Hudson Bay, Canada. *Environmental Science and Technology*, **43**, 2254-2261.
- King, J.W., Banerjee, S.K., Marvin, J., 1983. A new rock magnetic approach to selecting sediments for geomagnetic paleointensity studies: application to paleointensity for the last 4000 years. *Journal of Geophysical Research* **88**, 5911–5921.
- Kuzyk, Z.A., Macdonald, R.W., Granskog, M.A., Scharien, R.K., Galley, R.J., Michel, C., Barber, D., Stern, G., 2008. Sea ice, hydrological, and biological processes in the Churchill River estuary region, Hudson Bay. *Estuarine, Coastal and Shelf Science*, **77**, 369–384.

- Kuzyk, Z. Z. A., Macdonald, R. W., Johannessen, S. C., Gobeil, C., Stern, G. A., 2009. Towards a sediment and organic carbon budget for Hudson Bay. *Marine Geology*, 264, 190-208.
- Lajeunesse, P., St-Onge, G., 2008. The subglacial origin of the Lake Agassiz-Ojibway final outburst flood. *Nature Geoscience*, 1, 184-188.
- Liu, Q., Roberts, A. P., Larrasoana, J. C., Banerjee, S. K., Guyodo, Y., Tauxe, L., Oldfield, F., 2012. Environmental magnetism: principles and applications. *Reviews of Geophysics*, 50, 1-50.
- Macklin, M. G., Lewin, J., 2003. River sediments, great floods and centennial-scale Holocene climate change. *Journal of Quaternary Science* 18(2), 101-105.
- Manitoba Wildlands, 2005. The Hydro Province: Manitoba's Hydroelectric Complex.
- Meyers, P.A., 1997. Organic geochemical proxies of paleoceanographic, paleolimnologic, and paleoclimatic processes. *Organic Geochemistry* 27, 213–250.
- Mulder, T., Syvitski, J. P. M., 1995. Turbidity currents generated at rivermouths during exceptional discharges to the world oceans, *Journal of Geology*, v. 103, p. 285–299, doi:10.1086/629747.
- Mulder, T., Syvitski, J. P. M., Migeon S., Faugères, J.-C., Savoye, B., 2003. Hyperpycnal turbidity currents: Initiation, behavior and related deposits: A review, in E. Mutti, G. S. Steffens, C. Pirmez, M. Orlando, and D. Roberts, eds., *Turbidites: Models and problems*. *Marine and Petroleum Geology*, Special Issue 20, no. 6–8, p. 861–882.
- Mulder, T., and Chapron E., 2010, Flood deposits in continental and marine environments: Character and significance, in R. M. Slatt and C. Zavala, eds., *Sediment transfer from shelf to deep water—Revisiting the delivery system: AAPG Studies in Geology* 61, p. 1–30.
- Newbury, R. W., McCullough, G. K., Hecky, R. E., 1984. The Southern Indian Lake impoundment and Churchill River diversion. *Canadian Journal of Fisheries and Aquatic Sciences* 41: 548–557.
- North/South Consultants Inc., 2012. Limestone generating station: aquatic environment monitoring programs. A synthesis of results from 1985 to 2003.
- Parsons, J. D., Bush, J. W. M., Syvitski, J. P. M., 2001. Hyperpycnal plume formation from riverine outflows with small sediment concentrations: *Sedimentology*, v. 48, p. 465–478.
- Poff, N. L., Olden, J. D., Merritt, D. M., Pepin, D. M., 2007. Homogenization of regional river dynamics by dams and global biodiversity implications. *Proceedings of the National Academy of Sciences*, 104: 14, 5732-5737.

- Prinsenberg, S. J., 1980. Man-made changes in the freshwater input rates of Hudson and James Bays. *Canadian Journal of Fisheries and Aquatic Sciences*, **37**: 1101-1110.
- Prowse, T. D., 1993. Suspended sediment concentration during river ice breakup. *Canadian Journal of Civil Engineering*, **20**, 872-875
- Prowse, T. D., 1994. Environmental significance of ice to streamflow in cold regions. *Freshwater Biology*, **32**, 241-259.
- Reimer, P. J., Bard, E., Bayliss, A., Beck, J. W., Blackwell, P. G., Bronk-Ramsey, C., Buck, C. E., Cheng, H., Edwards, R. L., Friedrich, M., Grootes, P. M., Guilderson, T. P., Haflidason, H., Hajdas, I., Hatté, C., Heaton, T. J., Hoffman, D. L., Hogg, A. G., Hughen, K. A., Kaiser, K. F., Kromer, B., Manning, S. W., Niu, M., Reimer, R. W., Richards, D. A., Scott, E. M., Southon, J. R., Staff, R. A., Turney, C. S. M., van der Plicht, J., 2013. IntCal13 and Marine13 Radiocarbon Age Calibration Curves 0–50,000 Years cal BP. *Radiocarbon*, **55**, No 4.
- Rosenberg, D.M., Chambers, P.A., Culp, J.M., Franzin, W.G., Nelson, P.A., Salki, A.G., Stainton, M.P., Bodaly, R.A., Newbury, R.W., 2005. Chapter 19: Nelson and Churchill River Basins. In: Benke, A.C., Cushing, C.E. (Eds.), *Rivers of North America*. Elsevier Academic Press, Oxford, pp. 853–901.
- Sella, G. F., Stein, S., Dixon, T. H., Craymer, M., James, T. S., Mazzotti, S., Dokka, R. K., 2007. Observation of glacial isostatic adjustment in “stable” North America with GPS. *Geophysical Research Letters*, vol. 34, L02306, doi:10.1029/2006GL027081.
- Starkel, L., 2002. Change in the frequency of extreme events as the indicator of climatic change in the Holocene (in fluvial systems). *Quaternary International*, **91**, 25-32.
- Starkel, L., 2011. Present-day events and the evaluation of Holocene palaeoclimatic proxy data. *Quaternary International*, **229**, 2-7.
- Stewart, D. B., Lockhart, W. L., 2005. An overview of the Hudson Bay Marine Ecosystem. *Canadian Technical Report of Fisheries and Aquatic Sciences* no. 2586.
- St-Jacques, J-M., Sauchyn, D. J., Zhao, Y., 2010. Northern Rocky Mountain streamflow records : Global warming trends, human impacts or natural variability? *Geophysical Research Letters*, **37**, L06407, doi:10.1029/2009GL042045.
- Stoner, J. S., Channell, J. E. T., Hillaire-Marcel, C., 1996. The magnetic signature of rapidly deposited detrital layers from the deep Labrador Sea: Relationships to North Atlantic Heinrich Layers, *Paleoceanography*, **11**, 309–325, doi:10.1029/96PA00583.
- Stoner, J. S., St-Onge, G., 2007. Magnetic Stratigraphy in Paleoceanography: Reversals, Excursions, Paleointensity, and Secular Variation. *Developments in Marine Geology*, **1**, 99-138.

- St-Onge, G., Hillaire-Marcel, C., 2001. Isotopic constraints of sedimentary inputs and organic carbon burial rates in the Saguenay Fjord, Quebec. *Marine Geology*, **176**: 1-22.
- St-Onge, G., Mulder, T., Piper, D.J.W., Millaire-Marcel, C., Stoner, J.S., 2004. Earthquake and flood induced turbidites on the Saguenay Fjord (Québec): a Holocene paleoseismicity record. *Quaternary Science Reviews* **23**, 283–294.
- St-Onge, G., Lajeunesse, P., 2007. Flood-induced turbidites from northern Hudson Bay and Western Hudson Strait : a two-pulse record of Lake Agassiz final outburst flood? V. Lykousis, D. Sakellariou and J. Locat (eds.), Submarine Mass Movements and Their Consequences, 129–137.
- St-Onge, G., Mulder, T., Francus, P., Long, B., 2007. Continuous physical properties of cored marine sediment. In: Hillaire-Marcel, C., deVernal, A. (Eds.), Proxies in Late Cenozoic Paleoceanography (*Developments in Marine Geology*), vol. 1. Elsevier, pp. 99–138.
- St-Onge, G., Chapron, E., Mulsow, S., Salas, M., Viel, M., Debret, Foucher, A., Mulder, T., Winiarski, T., Desmet, M., Costa, P. J. M., Ghaleb, B., Jaouen, A., Locat, J., 2012. Comparison of earthquake-triggered turbidites from the Saguenay (Eastern Canada) and Reloncavi (Chilean margin) Fjords: implications for paleoseismicity and sedimentology. *Sedimentary Geology* **243–244**, 89-107.
- Stuiver, M., Reimer, P.J., Reimer, R.W., 2005. Online Radiocarbon Calibration Program CALIB 5.0.2. <http://calib.qub.ac.uk/calib/>.
- Syvitski, J.P.M., Vörösmarty, C.J., Kettner, A.J., Green, P., 2005. Impact of humans on the flux of terrestrial sediment to the global coastal ocean. *Science* **308**, 376–380.
- Tauxe, L., Mullender, T.A.T., Pick, T., 1996. Potbellies, wasp-waists, and superparamagnetism in magnetic hysteresis. *Journal of Geophysical Research* **101**, 571–583.
- Tauxe, L., 2010. Applied rock (environmental) magnetism. In Essentials of paleomagnetism. Berkeley : University of California Press.
- Valiela, I., Bartholomew, M., Giblin, A., Tucker, J., Harris, C., Martinetto, P., Otter, M., Camilli, L., Stone, T., 2014. Watershed Deforestation and Down-Estuary Transformations Alter Sources, Transport, and Export of Suspended Particles in Panamanian Mangrove Estuaries. *Ecosystems*, **17**, 96-111.
- Vannièvre, B., Magny, M., Joannin, S., Simonneau, A., Wirth, S. B., Hamann, Y., Chapron, E., Gilli, A., Desmet, M., Anselmetti, F. S., 2013. Orbital changes, variation in solar activity and increased anthropogenic activities: controls on the Holocene flood frequency in the Lake Ledro area, Northern Italy. *Climate of the Past*, **9**, 1193-1209.

- Vörösmarty, C. J., Meybeck, M., Fekete, B., Sharma, K., Green, P., Syvitski, J. P. M., 2003. Anthropogenic sediment retention: major global impact from registered river impoundments. *Global and Planetary Change*, 39, 169-190.
- Werritty, A., Paine, J. L., Macdonald, N., Rowan, J. S., McEwen, L. J., 2006. Use of multi-proxy flood records to improve estimates of flood risk: Lower River Tay, Scotland. *Catena*, 66, 107-119.
- Yang, Z., Wang, H., Saito, Y., Milliman, J. D., Xu, K., Qiao, S., Shi, G., 2006. Dam impacts on the Changjiang (Yangtze) River sediment discharge to the sea: The past 55 years and after Three Gorges Dam. *Water Resources Research*, 42, W04407, 1-10.
- Zhang, D., 2000. *Flux de radio-isotopes à courtes périodes dans les bassins marins marginaux de l'est canadien*. Thèse de doctorat 193 p, Université du Québec à Montréal, Montréal, QC Canada.

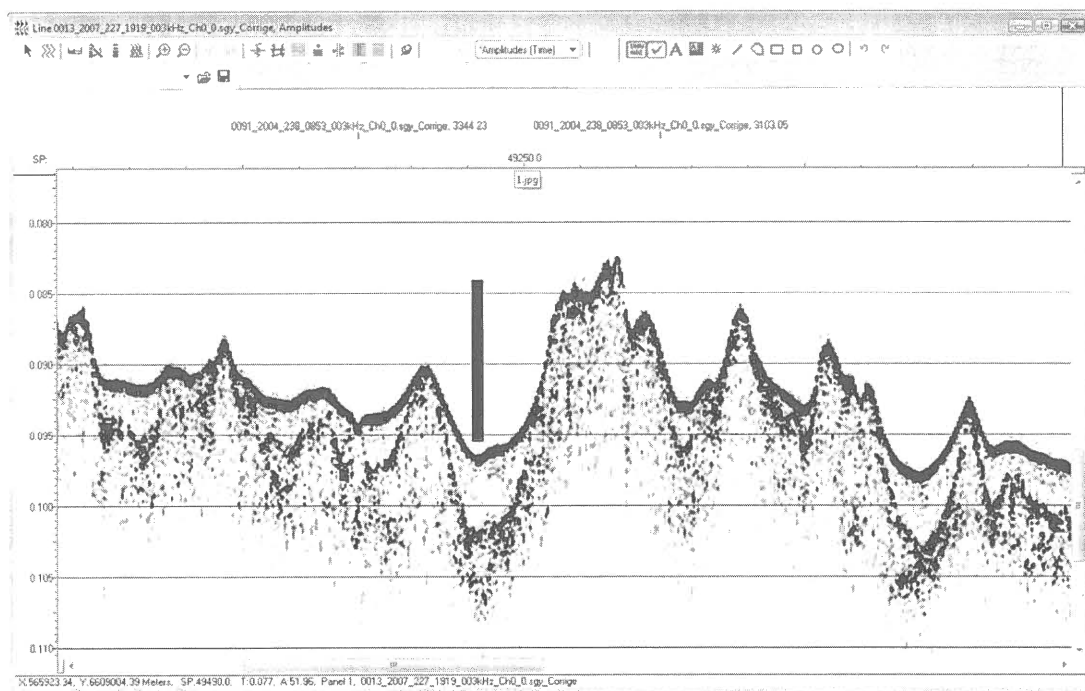
## ANNEXE 1

### COORDONNÉES D'ÉCHANTILLONNAGE ET LEVÉS SISMIQUES

*Station PRAD121-772*

	Coordonnées ( $^{\circ}$ -min-déc)		Coordonnées ( $^{\circ}$ -déc)		Prof. (m)
	Latitude	Longitude	Latitude	Longitude	
Coord. prévues	59°34,692' N	091°48,966' O	59,5782°	- 91,8161°	122,5
Carottier à boîte	59°34,710' N	091°48,950' O	59,5785°	-91,8158°	129
Carottier à gravité	59°34,709' N	091°48,963' O	59,5785°	-91,8160°	131

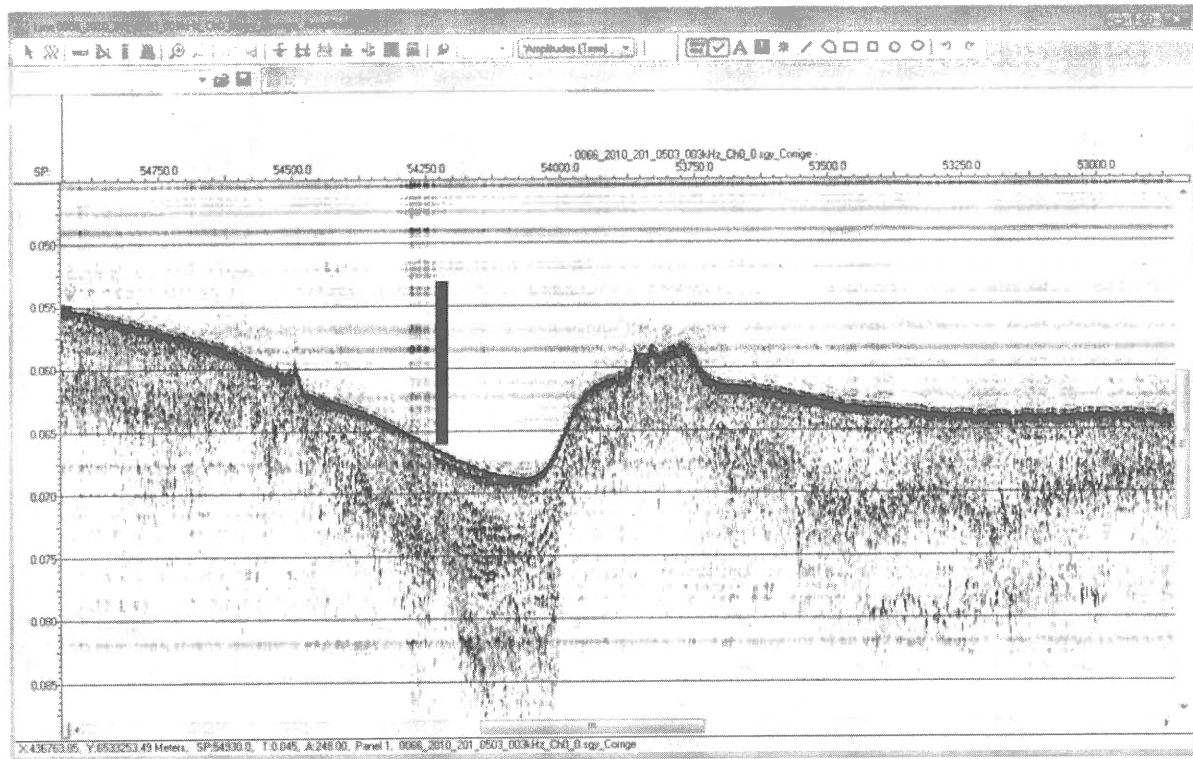
Levé sismique # 2007-227-1919 (station 772)



*Station PRAD121-776*

	Coordonnées (°-min-déc)		Coordonnées (°-déc)		Prof. (m)
	Latitude	Longitude	Latitude	Longitude	
Coord. prévues	58°58,368' N	094°05,896' O	58,9728°	-94,09826°	51
Carottier à boîte	58°58,342' N	094°05,899' O	58,9724°	-94,0983°	49
Carottier à gravité	58°58,345' N	094°05,919' O	58,9724°	-94,0986°	49.5

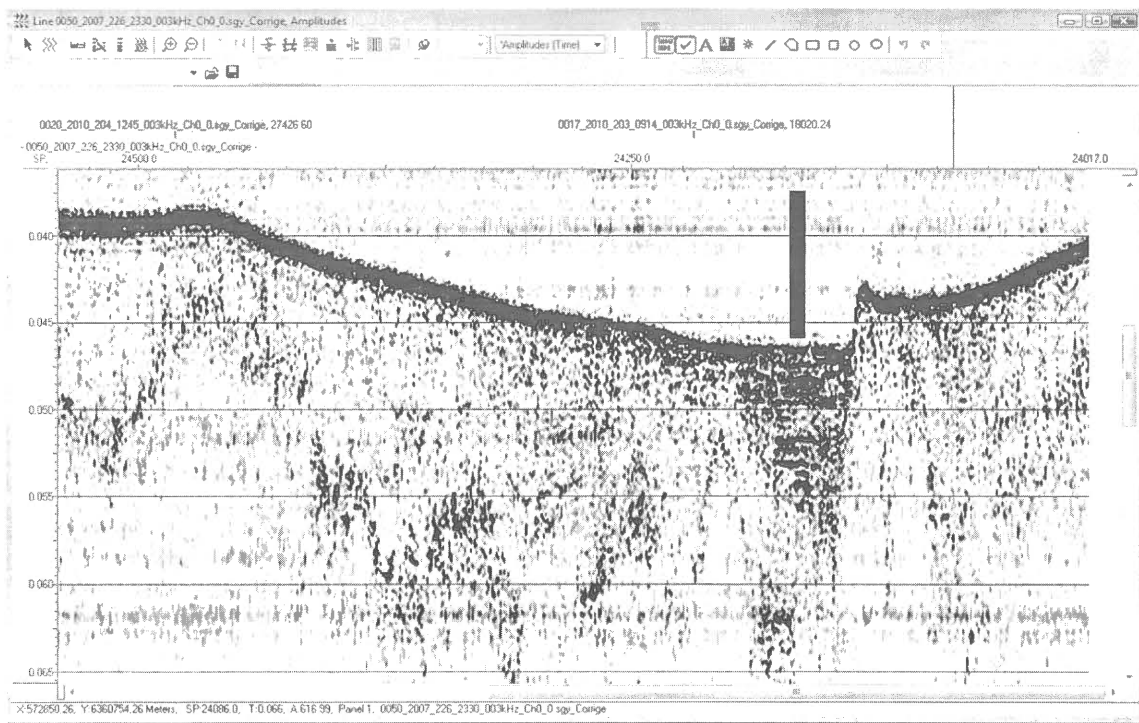
Levé sismique # 2010-201-0503 (station 776)



*Station PRAD121-778*

	Coordonnées (°-min-déc)		Coordonnées (°-déc)		Prof. (m)
	Latitude	Longitude	Latitude	Longitude	
Coord. prévues	57°23,346' N	091°47,832' O	57,3891°	- 91,7972°	35
Carottier à boîte	57°23,359' N	091°47,839' O	57,3893°	-91,7973°	37,5
Carottier à gravité	57°23,377' N	091°47,818' O	57,3896°	-91,7970°	37

Levé sismique # 2007-226-2330 (station 778)



*Station PRAD121-780*

	Coordonnées (°-min-déc)		Coordonnées (°-déc)		Prof. (m)
	Latitude	Longitude	Latitude	Longitude	
Coord. prévues	57°24,426' N	091°43,614' O	57,4071°	-91,7269°	50
Carottier à boîte	57°24,422' N	091°43,635' O	57,4070°	-91,7272°	48
Carottier à gravité	57°24,356' N	091°43,726' O	57,4059°	-91,7288°	49

Levé sismique # 2010-203-0914 (station 780)

